

Authors Response

Referee 1 – Anonymous

Overview:

Widiyanto et al. conducted field surveys of the 22 Dec 2018 Anak Krakatau volcano tsunami along the coastlines of Sunda Strait and reported wave runup distribution. They also collected sediment samples and performed tsunami deposit analysis.

I believe that this is an important study and the results are very useful. The manuscript reads well; its figures have good qualities and the structure of the manuscript is appropriate. However, I found some unclear points in the manuscript that needs to be corrected before publication. The details of runup survey are unclear and I made comments to help authors to correct it. Also the manuscript needs to compare its results with published papers on the Anak Krakatau tsunami and explain how this work connects with existing literature.

My recommendation is “Moderate Revision” with following comments. I encourage the authors to do the revisions quickly and resubmit soon in order to publish the paper earlier.

Response to overview:

We would like to thank Referee 1 for encouraging comments and constructive suggestions towards improving our manuscript. We summarize comments from Referee 1, author’s response, and author’s changes in manuscript as follows. Changes in manuscript will be available in marked-up/ revised manuscript if we have a chance to revise the manuscript.

Comment 1:

Page 2, Line 13: please show two locations “Merak” and “Bakahueni” in Figure 1.

Response 1:

Thanks for suggestion. Merak and Bakahueni are ferry ports with crowded traffic. They are important place to show. We add legends in Figure 1 in mark-up manuscript to show the two locations.

Comment 2:

P2, L1-9: in this part of introduction, I think it would be very useful if you report the two recently published papers on the same event. They are:

Muhari, A., Heidarzadeh, M., Susmoro, H., Nugroho, H.D., Kriswati, E., Supartoyo, Wijanarto, A.B., Imamura, F., Arikawa, T. (2019). The December 2018 Anak Krakatau volcano tsunami as inferred from post-tsunami field surveys and spectral analysis. *Pure and Applied Geophysics*, <https://doi.org/10.1007/s00024-019-02358-2>.

Heidarzadeh, M., Ishibe, T., Sandanbata, O., Muhari, A., Wijanarto, A.B. (2020). Numerical modeling of the subaerial landslide source of the 22 December 2018 Anak Krakatoa volcanic tsunami, Indonesia. *Ocean Engineering*, 195, <https://doi.org/10.1016/j.oceaneng.2019.106733>.

You could say like this: “The numerical modelling of the Dec 2018 Anak Krakatau tsunami was performed by Heidarzadeh et al. (2020) while Muhari et al. (2019) conducted field surveys of this event to record tsunami runup along the coasts of Sunda Strait”.

Response 2:

Thanks for suggestion. We report the two papers in part of introduction, and add them in part of reference belongs to marked-up manuscript.

Change in manuscript:

The numerical modelling of the December 2018 Anak Krakatau tsunami was performed by Heidarzadeh et al. (2020) while Muhari et al. (2019) conducted field surveys of this event to record tsunami runup along the coasts of Sunda Strait.

Comment 3:

P3, L36: here please clarify which coastline? We have two coastlines which are High Tide Coastline (HTC) and Low Tide Coastline (LTC). You measured runup based on HTC or LTC? This is very important to clarify.

Response 3:

We measure based on the coastline of measurement time. The numbers shown in the manuscript version 1 were original measurement values. Now, we correct them for tide using WXTide version 47 software. Tsunami arrival times are determined based on tidal record that show tsunami waveform. Four tidal gauge record were obtained from Geospatial Information Agency, Indonesia. They are Marina Jambu, Ciwandan, Panjang and Kota Agung. Or we can use the tide gauge data in article by Heidarzadeh (2020) which is published officially.

Change in manuscript:

The runup was measured by determining the height difference between the highest point of sea water rise onto land and the coastline. Runup is influenced by the characteristics of the ground surface and slope. The measurement results from our field surveys show that runup ranged from 1 to 9 m (Table 1 and Fig. 1). The values in the table and figure has been corrected for tide to obtain elevation from sea level at time of tsunami.

Comment 4:

P3, L13-16: here you talk about runup measurements; but you do not explain about tidal level corrections. The tide level at the time of actual tsunami was different from tidal level at the time of surveys. Please explain about this and the corrections that you made.

Response 4:

The numbers appear in the manuscript version 1 especially in Table 1 and Figure 1 were original numbers come from measurement. We have not corrected them for tide therefore we need to correct them using tidal levels. We use WXTide version 47 software to correct it. The station we use is Ciwandan, Serang, and Teluk betung tidal gauge station. The corrected values will be shown in mark-up manuscript if this process continue to next stage.

Change in manuscript:

Measurements of runup and inundation were conducted using conservative terrestrial surveying methods with optical and laser devices (e.g., total stations, handheld GPS devices, and laser distance meters). We measured run-up and inundation based on coastline at the time of survey. Run-up were corrected to calculate heights above sea level because the tide level at the time of actual tsunami was different from tidal level at the time of surveys. We use WXTide software version 4.7 for correcting elevation. Elevation values of each survey site were corrected with the nearest tidal gauge available. We used 3 tide station in Ciwandan, Labuhan and Teluk Betung.

Comment 5:

P3, L34-40: please compare your runup heights with those of Muhari et al. (2019) [Pure and Applied Geophysics, <https://doi.org/10.1007/s00024-019-02358-2>] and explain why Muhari et al. reported maximum runup height of 13 m but you report max runup of 8? Is that because you did not survey same points? Please clarify.

Response 5:

Thanks for recommendation. Yes right. The difference is because we measured in different points. Our maximum run-up point (Cagar Alam) is located very far from maximum run-up point (Tanjungjaya) belongs to Muhari et al. Actually, we also have a measurement point near Muhari et al. measured. It is site Tanjungjaya-2 or local people call it Cipenyu Beach. The height of run-up is 9 m, we add it in marked-up manuscript and become the highest run-up in our survey. Nevertheless, this value is still significant different with Muhari et al. since we measure in flat valley part of Cipenyu Beach while Muhari et al. measured in hilly coast of Cipenyu Beach.

Change in manuscript:

The measurement results from our field surveys show that run-up ranged from 1 to 9 m (Table 1 and Fig. 1). A runup height of about 1 m was found in many locations, at which no damage was found. The highest runup was found at the Tanjung Jaya 2, Cagar Alam, and Kunjir sites, with heights of 9.0, 7.8, and 7.7 m respectively. Site Tanjungjaya 2 is located in Cipenyu Beach. Muhari et al. (2019) reported maximum runup height of 13 m in area around Tanjungjaya/Cipenyu Beach as well. This value is significant different with our maximum run-up since we measure in flat valley part of Cipenyu Beach while Muhari et al. measured in hilly coast of Cipenyu Beach.

Comment 6:

P3, L34-40: Here also please compare your surveyed runup heights with published tide gauge records of Heidarzadeh et al. (2020) [Ocean Engineering, 195, <https://doi.org/10.1016/j.oceaneng.2019.106733>]. For example, your runup heights how many times are larger than tide gauge heights reported by Heidarzadeh et al.? this information can be very useful.

Response 6:

Thanks for the interesting recommendation. We compare our surveyed runup heights with published tide gauge records of Heidarzadeh et al. (2020) [Ocean Engineering, 195, <https://doi.org/10.1016/j.oceaneng.2019.106733>]. We use 3 tide gauges from the paper: Ciwandan, Marina Jambu and Panjang. Others (Kota Agung, Bengkurat, Binuangeun) are too far from our survey site. We read that maximum amplitudes at Ciwandan, Marina Jambu, and Panjang are 1.15 m, 2.8 m, and 1.25 m respectively. Ciwandan tide gauge is used to evaluate runup heights at site Karangsuraga, Pasauran, Sukarame and Pejamben. It results in average runup heights 4 times larger than amplitude at tide gauge heights. Note that the sites are relatively far from the tide gauge. Marina Jambu is used to evaluate runup heights at sites Sukamaju, Karang Sari, Tanjungjaya 1, Tanjunglesung (1,2,3), Tanjungjaya 2, Banyuasih, Kertajaya Sumur, Cagar Alam. It results in average runup heights 1.15 times larger than amplitude at tide gauge. Panjang tide gauge is used to evaluate sites of Bumiwaras, Wayurang 1, Wayurang 2, Kotaguring, Sukaraja, and Kunjir. It results in average runup heights of 3.1 times larger than amplitude at tide gauge.

Change in manuscript:

Our surveyed runup heights are compared with published tide gauge records of Heidarzadeh et al. (2020). Three tide gauges from the article (Ciwandan, Marina Jambu and Panjang) are used. Maximum amplitudes at Ciwandan, Marina Jambu, and Panjang are 1.15 m, 2.8 m, and 1.25 m respectively. Ciwandan tide gauge is used to evaluate runup heights at site Karangsuraga, Pasauran, Sukarame and Pejamben. Marina Jambu tide gauge is used to evaluate runup heights at sites Sukamaju, Karang Sari, Tanjungjaya 1, Tanjunglesung (1,2,3), Tanjungjaya 2, Banyuasih, Kertajaya Sumur, Cagar Alam. Besides, Panjang tide gauge is used to evaluate sites of Bumiwaras, Wayurang 1, Wayurang 2, Kotaguring, Sukaraja, and Kunjir. It is indicated that averaged runup heights of each site associated with the tide gauge are 4 times, 1.15 times, and 3.1 times larger than maximum amplitude at the Ciwandan, Marina Jambu, and Panjang respectively. The sites are relatively far from the tide gauge.

Comment 7:

P4, L1: please show location "Sumur" in Figure 1.

Response 7:

Alright, we show location Sumur in Figure 1 and will appear in marked-up manuscript.

Comment 8:

P4, L6: same comment as before for coastline; HTC or LTC?

Response 8:

We measured inundation distance based on the coastline of surveys time. The numbers shown in the manuscript version 1 were original measurement values. Correct values with tidal data will be shown in marked-up manuscript.

Change in manuscript:

The distance from the runup point to the coastline is defined as the inundation distance (IOC Manuals and Guides No. 37, 2014). This distance can be easily obtained using a distance measurement instrument or GPS. We used total station for this purpose. The coastlines elevation in our survey were corrected with tide elevation of several tide gauge in Sunda Strait. The results of our field measurements show that the inundation distance ranged from 10 to 290 m (Table 1 and Fig. 1).

Comment 9:

P4, L3; 250 m. Add "m".

Response 9:

Thanks for thorough review, we add "m" in the value.

Change in manuscript:

The topography is relatively flat but suddenly rises at a distance of about 250 m from the coastline due to a long hill.

Comment 10:

how much is the value of gamma?

Response 10:

Gamma is a comparison factor between uprush time and total uprush plus backwash time. In our paper, gamma varies from 0.03365 to 0.889192. We use some assumption, e.g. velocity of tsunami flow 5-6 m/s and period from the time of first wetting to final drying of inundated ground 2-5 hours. They depend on length of inundation and morphology.

Comment 8:

Figure 1: Please make the distance scale more clear and visible.

Response 8:

OK, thanks. We modify it in order to be visible and clearer. It will be ready in marked-up manuscript.

Comment 9:

Figure 2: please increase fontsize. Most texts cannot be read.

Response 9:

Alright, we increase the font size in order to be readable. It will ready in marked-up manuscript.

Comment 10:

Figure 3: please add name of each location after the letters "a", "b", ; : :.in each panel.

Response 10:

Thanks for your suggestion to make the figure clearer. Location name for a is Carita Beach ; b = Tanjung Lesung; c = Cagar Alam; d = Cagar Alam; e = Tanjung Lesung; f = Tanjung Lesung; g = Cagar Alam.

Comment 11:

Figure 4; please add some location names in this figure'; for example location names of 2, 4, 10 and 14.

Response 11:

Thanks. Actually, there are location names in Figure 4, but they are not readable. We make them more visible and we add other location names and site number to Figure 4. Location name of 2 is Pasauran; 4 = Pejamben; 10 = Tanjung Lesung; 14 = Cagar Alam.

Comment 12:

Figure 5: Please add location name in each panel.

Response 12:

Thanks for your suggestion. We add the location name to Figure 5 while the coordinates of the test pits can be seen in Table 2. The location name of upper left panel is Cagar Alam, upper right is Sukarame, lower left is Karangsuraga, and lower right is Cagar alam. These name will appear in marked-up manuscript.

Comment 13::

Figures 6 and 7: please combine these two figures to only one figure with two panels.

Response 13:

Thanks for your suggestion. One figure with two panels will make the manuscript more effective and efficient. We combine Figure 6 and 7 and will be ready in marked-up manuscript.

Comment 14:

Table 1: in column 3, please add time as well. You have only date now. What time of the day? This is very important because we can see how tidal status was at the time of your survey.

Response 14:

We recorded the times of survey for each site. We add them in column 3 of Table 1 in marked-up manuscript.

Authors Response

Referee 2 – Prof. Ahmed Cevdet Yalciner

The authors conducted a field survey a month after the 22 December 2018 Anak Krakatau tsunami event. The paper presented and discussed the measurements of runup height, inundation distance, tsunami direction, and sediment characteristics at selected sites. The followings are my comments on the manuscript.

Major comment and recommendation:

Page 1, Lines 8-9: You had better rewrite the sentence “The affected area of the tsunami included a coastal area located at the edge of Sunda Strait, Indonesia.” in such a way “The tsunami affected the coastal areas located at the edge of Sunda Strait, Indonesia.”

Response 1:

Thanks for correction. We change the sentence according to your recommendation.

Change in manuscript:

A tsunami caused by a flank collapse of the southwest part of the Anak Krakatau volcano occurred on December 22, 2018. The tsunami affected the coastal areas located at the edge of Sunda Strait, Indonesia. To gain an understanding of the tsunami event, field surveys were conducted a month after the incident.

Page 1, Lines 13-14: The sentence is grammatically incorrect. “Tsunami propagated radially from its source and arrived in coastal zone with direction was between 25° and 350° from North.”. Please rewrite.

Response 2:

Thanks for correction.

Change in manuscript:

The tsunamis propagated radially from Anak Krakatau and reached the coastal zone with direction between 25° and 350° from North.

Page 1, Lines 26-27: There is an incorrect statement in the sentence “The southwestern slope of the mountain experienced a landslide below the sea surface that resulted in..” because the landslide not only occurred below the sea surface but also there is a subaerial part of the landslide.

Response 3:

Thanks for the correction. We remove “below the sea surface”.

Change in manuscript:

The southwestern slope of the mountain experienced a landslide that resulted in the movement of sea water, which propagated to land in the form of a tsunami wave.

Page 2, Lines 12-15: Any reference for such kind of information “It connects the two main islands of Java and Sumatra, whose population accounts for 79% of Indonesia's population. About 6.9 million people live in the coastal area of the strait in Banten Province and Lampung Province.” OR “The strait, between Merak and Bakauheni, is the busiest inter-island crossing in Indonesia, with more than 50,000 passengers/day and more than 20,000 vehicles/day.”

Response 4:

We add the references for this part:

BPS-Statistics Indonesia: Statistical Yearbook of Indonesia 2019, Jakarta, 2019.

BPS-Statistics of Banten Province: Banten Province in Figures 2019, Serang, 2019.

BPS-Statistics of Lampung Province: Lampung Province in Figures 2019, Bandar Lampung, 2019.

Dirjen Perhubungan Darat: Perhubungan Darat dalam Angka 2018, Jakarta, 2019

Soeriaatmadja, W.: Indonesia plans traffic system for busy Sunda Strait, available at <https://www.straitstimes.com/asia/se-asia/indonesia-plans-traffic-system-for-busy-sunda-strait> (last access, 10 January 2020), 2020.

Change in manuscript:

It connects the two main islands of Java and Sumatra, whose population accounts for 79% of Indonesia's population (BPS-Statistics Indonesia, 2019). About 6.9 million people live in the coastal area of the strait in Banten Province and Lampung Province (BPS-Statistics of Banten Province, 2019; BPS-Statistics of Lampung Province, 2019). The strait, between Merak and Bakauheni, is the busiest inter-island crossing in Indonesia, with 17.824.392 passengers and 4.218.548 vehicles in 2018 (Dirjen Perhubungan Darat, 2019). The strait is also an international route for large ships. It is the second-most crowded waterway after Malacca Strait, with 70,000 vessels a year passing it (Soeriaatmadja, 2016).

Page 4, Lines 14-15: "A relatively long inundation (284.2 m) was also found at Tanjungjaya 2, a site 15 with a relatively high runup." Any information on the steepness of the slope which can justify the situation given in this information?

Response 5:

Site Tanjungjaya 2 has different characteristics from other sites. This site is in the form of a valley plain with a small stream. Slope in the valley is relatively flat and suddenly changes sharply in hilly areas within 250-300 m from coastline. The run-up point that we recorded is located on the slope change from mild to steep. These flat and sharp areas have slopes of approximately 0.025 and 0.06, respectively. Local people call this area as Cipenyu Beach. This is a sandy beach flanked by cliffs or hilly beaches.

Change in manuscript:

A relatively long inundation (284.2 m) was also found at Tanjungjaya 2, a site with a relatively high runup. This site is in the form of a valley plain with a small stream. Slope in the valley is relatively flat and suddenly changing steeply in hilly areas within 250-300 m from coastline. The run-up point we recorded is located on the slope change from mild to steep. These mild and steep areas have slopes of approximately 0.025 and 0.06, respectively. Local people call this area as Cipenyu Beach. This is a sandy beach flanked by cliffs or hilly beaches. Fortunately, not many people live around this site other than at a resort complex, which suffered severe damage.

Page 6, Lines 12-13: "We identified boulders moved by a tsunami wave and runup at three survey sites based on information from eyewitnesses and their physical state." The phrase in bold is redundant.

Response 6:

Thanks for the correction. We delete the phrase in bold.

Change in manuscript:

We identified boulders moved by a tsunami wave and runup at three survey sites based on information from eyewitnesses.

Page 6, Lines 12-13: "In addition, from the physical criteria given by Morton et al. (2007) and Paris et al. (2010), it was most likely that the boulders were moved by the tsunami." It is needed to mention a little bit about the "physical criteria" mentioned in this sentence and how you related it to your case.

Response 7:

Thanks for recommendation. We conclude that the boulder was transported by tsunami mainly based on eyewitness information. We add a little bit about the "physical criteria" by Morton et al. (2007) and Paris et al. (2010) as we write in change manuscript here.

Change in manuscript:

Eyewitnesses said that these boulders were in new positions after the tsunami. In addition, from the physical criteria given by Morton et al. (2007) and Paris et al. (2010), it was most likely that the boulders were moved by the tsunami. One of criteria by Morton et al. (2007) we found in this site is a relatively thin (average < 25 cm) bed composed of normally graded sand consisting of a single structureless bed or a bed with only a few thin layers. Sediment thickness around the boulder is very thin. Paris et al. (2010) reported regarding boulder and fine sediment transport and deposition by the 2004 tsunami that most of the sediments deposited on land came from offshore, from fine sands to coral boulders, and with very high values of shear velocity (>30 cm/s). The boulder we found came from nearshore and a part of the boulder was submerged. We estimate that high shear velocity should occur to transport it. It was most possible by 22 December 2018 tsunami.

Page 6, Lines 33-34: "and ρ_w is the density of sea water." Unit is missing. "The velocities were calculated **from Equation 3** to be $u \geq 4.5$ m/s and $u \geq 4.0$ m/s for the 10.4-ton (Fig. 8a) and 9.4-ton (Fig. 8b) boulders, respectively." If so, please add the highlighted words.

Response 8:

Thanks for correction and suggestion. Unit for density of sea water is kg/m^3 . Right, the velocities were calculated from Equation 3. We add the highlighted words.

Change in manuscript:

where μ is the friction coefficient, m is the boulder mass (kg), g is the gravitational acceleration, C_d is the drag coefficient, A_n is the area of the boulder projected normal to the flow (m^2), and ρ_w is the density of sea water (kg/m^3). The velocities were calculated **from Equation 3** to be $u \geq 4.5$ m/s and $u \geq 4.0$ m/s for the 10.4-ton (Fig. 8a) and 9.4-ton (Fig. 8b) boulders, respectively.

Page 7, Line 28: "...and the direction of the tsunami was between 25° and 350° **from North**." Better to add the highlighted words.

Response 9:

Thanks for the correction.

Change in manuscript:

The survey results revealed that the runup height ranged from 1 to 8 m, the inundation distance was 10 to 300 m, and the direction of the tsunami was between 25° and 350° **from North**.

It is better to explain the reasons (local morphological conditions, ground material, ground slope etc.) of the discrepancies between theoretical deposit limit and the measured deposit limit at the locations where they do not fit well such as Sukarame, Tanjungjaya 1 and Cagar Alam.

Response 10:

Thanks for your suggestion. The three location have morphological conditions may not ideal for applying the theoretical approach. Sukarame has beach scarp and tsunami flows across a stream around 90 m from coastline. Tanjungjaya 1 has also beach scarp and there is a sea wall (although not so high) that may block the sediment movement. Eventhough Tanjungjaya 1 has abundant material, low amplitude tsunami caused a few sand transport. Cagar alam has a relative bigger stream than Sukarame. In addition, Cagar Alam has dense vegetation since it is a national park.

Change in manuscript:

Fig. 7 shows the distance of measured sediment deposition and water runup compared to the distance of theoretical sediment deposition calculated using Eq. 1 and Eq. 2, the results are in good agreement. However, Sukarame, Tanjungjaya 1 and Cagar Alam do not fit well. The three location have morphological conditions may not ideal for applying the theoretical approach. Sukarame has beach scarp and tsunami flows across a stream around 90 m from coastline. Tanjungjaya 1 has also beach scarp and there is a sea wall, although not so high, that may block the sediment movement. Eventhough Tanjungjaya 1 has abundant material, low amplitude tsunami caused a few sand transport. Cagar Alam has a relative bigger stream than Sukarame. In addition, Cagar Alam has dense vegetation since it is a national park. The distance of area with significant sediment deposits caused

by the tsunami from the coast varied in the range of 15-200 m (average: 93 m) from the shoreline or 40%-90% (average: 67%) of the inundation distance.

Any information on the tidal situation of the area? Is there any detiding process performed on the measured values?

Response 11:

Yes, we have 4 tidal gauge data giving information on the tidal situation from the area. Our measured values shown in the manuscript version 1 are original values. We have not corrected the measured values in the manuscript version 1. We will show corrected values in mark-up manuscript if it continues to next stage. We use WXTide 47 software to correct the measured values. Tsunami arrival times are determined based on tidal record that show tsunami waveform. Four tidal gauge record were obtained from Geospatial Information Agency, Indonesia. They are Marina Jambu, Ciwandan, Panjang and Kota Agung.

Change in manuscript:

Measurements of runup and inundation were conducted using conservative terrestrial surveying methods with optical and laser devices (e.g., total stations, handheld GPS devices, and laser distance meters). We measured run-up and inundation based on coastline at the time of survey. Run-up were corrected to calculate heights above sea level at the time of the survey using WXTide software version 4.7. Elevation values of each survey site were corrected with the nearest tidal gauge available. We used 3 station in Ciwandan, Labuhan and Teluk Betung, for corrections.

In conclusion part especially, why needed to use past tense for some findings? They are still valid. For example, "The largest boulder **had (has)** a diameter of 2.7 m and a weight of 10.4 tons. From the boulder movement, the tsunami velocity at the ground surface **was (is)** estimated to be more than 4.5 m/s. Sand size statistics **were (are)** also given in this report. The sediment grain size ranged from very fine sand to boulders, with medium sand (diameter: 0.25-0.5 mm) and coarse sand (diameter: 0.5 -1.0 mm) being dominant. All sediment samples tested in the laboratory **had (has)** a well sorted distribution, indicating that the grain sizes were relatively uniform.

Response 12:

Thanks for correction regarding basic writing. We check throughout manuscript about it and revise as you suggest.

Change in manuscript:

The largest boulder **has** a diameter of 2.7 m and a weight of 10.4 tons. From the boulder movement, the tsunami velocity at the ground surface **is** estimated to be more than 4.5 m/s. Sand size statistics **are** also given in this report. The sediment grain size ranged from very fine sand to boulders, with medium sand (diameter: 0.25-0.5 mm) and coarse sand (diameter: 0.5 -1.0 mm) being dominant. All sediment samples tested in the laboratory **has** a well sorted distribution, indicating that the grain sizes are relatively uniform.

Figures and Typos:

Page 3, Line 13: "terrestrial" "terrestrial"

Response 13:

Thanks.

Change in manuscript:

Measurements of runup and inundation were conducted using conservative **terrestrial** surveying methods with optical and laser devices (e.g., total stations, handheld GPS devices, and laser distance meters).

Figure 3: Only places and arrows are shown in the pictures of Figure 3 which are not satisfactory for inferring the wave direction at these locations. Indication of the locations where each picture belongs to is necessary. Writing also the coordinates may be a good idea.

Response 14:

Thanks for comment and recommendation. We add the site names and coordinates. Fortunately, we recorded coordinates for each locations, for instance shown by Fig. 3a, a man was recording a coordinates on a fallen tree.

Fig 3a (105.829587° , -6.316732°) Pejamben

Fig 3b (105.652357° , -6.481177°) Tanjunglesung

Fig 3c 105.378817° , -6.674535° Cagar Alam

Fig 3d 105.378692° , -6.676228° Cagar Alam

Fig 3e 105.830286° , -6.316416° Pejamben

Fig 3f 105.829155° , -6.317243° Pasauran

Fig 3g 105.830011° , -6.316646° Pejamben

Fig 3h 105.379027° , -6.675038° Cagar Alam

We add them in mark-up manuscript

Change in manuscript:

Example



Figure 4 and Page-4, Lines 27-35: Can you please indicate the survey point IDs of the arrows shown in Figure 4 as well as the ones stated in these lines such as “Tanjung Lesung (sites 7-13)” or, for example, where is this Tanggamus area? Then, the statements in these lines on Page 4 will make sense while reading and looking at the figure.

Response 15:

Yes, we can put the point IDs for each arrows in Fig 4. Also add the position of location mentioned in Page 4 but not shown in Fig 4 such as Tanggamus, Sertung island and Indian Ocean. Thanks for kind recommendation.

Change in manuscript:

Figure 4 revised.

Page 4, Line 34: “Table 1 contains the quantity of tsunami wave direction arrived in coastal area.” Better rewrite this sentence in such a way “Tsunami wave direction from North arrived in coastal area is given/presented in Table 1 for the field survey sites.”

Response 16:

Thanks for your kindly correction.

Change in manuscript:

Tsunami wave direction from North arrived in coastal area is given in Table 1 for the field survey sites.

Page 4, Line 35: “north” → “North”, please correct this type of typos throughout the manuscript.

Response 17:

We correct them throughout the manuscript.

Change in manuscript:

“north” → “North”

Page 4 Line 30 need to revise

Page 4 Line 35 need to revise

Page 1 Line 14 already correct

Table 1 already correct

Page 5, Lines 3-4: “Prehistoric (paleo-) tsunamis have been identified from sediment deposits (Atwater 1992; Dawson and Shi 2000; Peters, Jaffe and Gelfenbaum 2007).” Is this sentence a general statement since it is not clear if it is a general statement or mentioning about a specific study for a region for example? Better rewrite the sentence as “Prehistoric (paleo-) tsunamis have been identified from sediment deposits in several/many studies/publications (Atwater 1992; Dawson and Shi 2000; Peters, Jaffe and Gelfenbaum 2007).”

Response 18:

Thanks for the suggestion. This is a general statement regarding studies on identification of prehistoric (paleo-) tsunamis from sediment deposits.

Change in manuscript:

Prehistoric (paleo-) tsunamis have been identified from sediment deposits **in several studies** (Atwater 1992; Dawson and Shi 2000; Peters, Jaffe and Gelfenbaum 2007).

Page 5, Line 16: “Four deposit pits were less than 50 m from the shoreline (11).” What is this 11 here?

Response 19:

Thanks for very thorough review. (11) should be (Figure 6). We used “cross-reference” menu in MS Word but it cause problem in process of converse to PDF file. We repair it.

Change in manuscript:

Four deposit pits were less than 50 m from the shoreline (Figure 6).

Page 5, Line 18: “...and created a deposit a short distance from the...” → “...and created a deposit **at** a short distance from the...”

Response 20:

Thanks for very thorough review.

Change in manuscript:

Another was at site 13 (Kertajaya Sumur), where high-density housing blocked the sediment transport and created a deposit **at** short distance from the shoreline.

Page 5, Line 23: “reconstructing **tsunamis** runup from sedimentary characteristics.”

Response 21:

Thanks for very thorough review.

Change in manuscript:

Soulsby et al. (2007) proposed a mathematical model for reconstructing **tsunami** runup from sedimentary characteristics.

Page 6, Line 24: “Other smaller chunks also moved.” → “Other smaller chunks **were** also moved.”

Response 22:

Thanks for correction.

Change in manuscript:

Other smaller chunks **were** also moved.

We would like to thank Prof Ahmed Cevdet Yalciner (Referee 2) for the constructive comments, very detail corrections, and recommendations towards improving our manuscript. We are improving our writing quality based on your kind suggestion. These comments are all valuable and very helpful for improving our paper. We appreciate that we have a chance to revise the manuscript as you recommend and to resubmit our manuscript will meet your approval.

Run-up, Inundation, and Sediment Characteristics of December 22 2018 Indonesia Sunda Strait Tsunami

Wahyu Widiyanto^{1,2}, Shih-Chun Hsiao¹, Wei-Bo Chen³, Purwanto B. Santoso², Rudy T. Imananta⁴, Wei-Cheng Lian¹

5 ¹Department of Hydraulic and Ocean Engineering, National Cheng Kung University, Tainan, 701, Taiwan

²Department of Civil Engineering, Universitas Jenderal Soedirman, Purwokerto, 53122, Indonesia

³National Science and Technology Center for Disaster Reduction, New Taipei City, 23143, Taiwan

⁴Meteorological, Climatological and Geophysical Agency (BMKG), Jakarta, 10720, Indonesia

Correspondence to: Shih-Chun Hsiao (schsiao@mail.ncku.edu.tw)

10 **Abstract.** A tsunami caused by a flank collapse of the southwest part of the Anak Krakatau volcano occurred on December 22, 2018. **The tsunami affected the coastal areas located at the edge of Sunda Strait, Indonesia.** To gain an understanding of the tsunami event, field surveys were conducted a month after the incident. The surveys included measurements of run-up height, inundation distance, tsunami direction, and sediment characteristics at 20 selected sites. The survey results revealed that the run-up height reached 9.2 m in Tanjungjaya and inundation distance 292.2 m was found at Site Cagar Alam, part of
15 Ujung Kulon National Park. **The tsunamis propagated radially from Anak Krakatau and reached the coastal zone with direction between 25° and 350° from North.** Sediment samples were collected at 27 points in tsunami deposits with a sediment thickness of 1.5-12 cm. The distance of the sediment deposit area from the coast was 40%-90% of the distance of the inundation caused by the tsunami. The highest elevation of deposits was 60%-90% of the highest run-up. Sand sheets were sporadic, highly variable, and highly influenced by topography. Grain sizes in the deposit area were finer than those at their sources. The sizes
20 ranged from fine sand to boulders, with medium sand and coarse sand being dominant. All sediment samples had a well sorted distribution. An assessment of the boulder movements indicates that the tsunami run-up had minimum velocities of 4.0-4.5 m/s.

1 Introduction

A tsunami took place in Sunda Strait on December 22, 2018, at 22:00 Western Indonesia Time (+7 UTC). It shocked the local
25 residents because it came without any warning signs, such as earthquake shocks. The source of the tsunami was the Anak Krakatau volcano, a sea mountain in the middle of Sunda Strait. **The southwestern slope of the mountain experienced a landslide that resulted in the movement of sea water, which propagated to land in the form of a tsunami wave.** When the tsunami reached land, its large energy caused a lot of damage and casualties. Records obtained from the Indonesian National Disaster Management Agency (Indonesian: Badan Nasional Penanggulangan Bencana, BNPB) show 430 deaths, 1015
30 collapsed houses, and a lot of other damage (e.g., seawalls, revetments, jetties, boats, and cars). The affected areas in Banten Province include Pandeglang and Serang Districts and those in Lampung Province include the regencies of South Lampung, Tanggamus, and Pesawaran.

Sunda Strait is home to the Krakatau (or Krakatoa) volcano. It is famous for the 1883 Krakatau eruption, which caused a 30-m tsunami that led to 36,000 fatalities and affected the Earth's climate and weather for several weeks, as reported by Verbeek
35 (1884). The 1883 eruption of Krakatau and the resulting tsunami have been widely discussed (e.g., Yokoyama 1987; Camus *et al.* 1992; Maeno and Imamura 2011; Paris *et al.* 2014). A young volcano called Anak Krakatau (Child of Krakatau) appeared above sea level in 1929. It grew to 338 m above sea level in September 2018. This very active volcano was the source of the tsunami discussed in the present study.

The generation of the tsunami that occurred on December 22, 2018, in Sunda Strait was triggered by the collapse of a flank in the southwest part of the Anak Krakatau volcano. Satellite imagery shows that the area of the body of the marine volcano that was lost was 64 hectares; the collapsed volume was estimated to be 150-180 million m³ (Kasbani, 2018). As a result of the collapse of some of the volcano's body, the volcano's height decreased from 338 to 110 m above sea level. The tsunami caused by the collapse of the Anak Krakatau flank was investigated by Giachetti et al. (2012). They used a numerical model to simulate an unstable flank collapse in the southwest part of Anak Krakatau. A hypothetical volume of 280 million m³ produces a wave with an initial height of 43 m on Sertung, Panjang, and Rakata islands that then spreads to the beaches in the western part of Java Island, including Merak, Anyer, Carita, Panimbang, and Labuhan, and Sumatra Island, reaching Bandar Lampung City. The actual area affected by the December 22 event is consistent with their model, but different in magnitude due to the use of the worst case scenario in the simulation. [The numerical modelling of the December 2018 Anak Krakatau tsunami was performed by Heidarzadeh et al. \(2020\) while Muhari et al. \(2019\) conducted field surveys of this event to record tsunami run-up along the coasts of Sunda Strait.](#)

Tsunamis in Sunda Strait are of great concern because the strait is important both locally and globally. It connects the two main islands of Java and Sumatra, whose population accounts for 79% of Indonesia's population (BPS-Statistics Indonesia, 2019). About 6.9 million people live in the coastal area of the strait in Banten Province and Lampung Province (BPS-Statistics of Banten Province, 2019; BPS-Statistics of Lampung Province, 2019). The strait, between Merak and Bakauheni, is the busiest inter-island crossing in Indonesia, with 17.824.392 passengers and 4.218.548 vehicles in 2018 (Dirjen Perhubungan Darat, 2019). The strait is also an international route for large ships. It is the second-most crowded waterway after Malacca Strait, with 70,000 vessels a year passing it (Soeriaatmadja, 2016). There are three industrial regions at the edge of the strait, namely Cilegon, Serang, and Tanggamus. There is also a special economic zone in this region, namely Tanjung Lesung. The beaches in the strait are a tourist destination. There are two UNESCO world heritage sites across from each other; one at the western tip of Java Island (Ujung Kulon National Park) and the other at the southern tip of Sumatra Island (Bukit Barisan Selatan National Park). Bandarlampung, which has a population of 1 million, is the provincial capital and faces the strait directly. Jakarta, the capital of the Republic of Indonesia, is relatively close to the strait. Post-tsunami field surveys were conducted to obtain data for future mitigation and development activities in the region. The surveys began exactly a month after the tsunami, January 22, and ended on January 28, 2019. Our team included people from Indonesia and Taiwan. We carried out measurements of the run-up height and inundation distance of the tsunami. In addition, we also identified flow directions and sediment deposits caused by the tsunami.

2 Study Area

The tsunami has had a serious impact on life in the surrounding area. The affected area covers the coastal area on the western tip of Java Island (Banten Province) and the southern tip of Sumatra Island (Lampung Province). Banten Province covers two districts, namely Serang and Pandeglang. Lampung Province covers South Lampung Regency and the provincial capital of Lampung, namely Bandar Lampung. Post-tsunami field surveys were conducted in these areas. We selected 20 sites for observation and measurement (Table 1 and Fig. 1). These sites are located along 140 km of coast on Java Island and 80 km of coast on Sumatra Island. Sites 13 and 14 were reached by boat because of the difficult land route.

Land use at these sites includes housing, agriculture, tourism, and a national park. Sites 1, 2, 4, 7, 8, 9, and 10 (Karangsugra, Pasauran, Pejamben, Tanjungjaya 1, and Tanjunglesung 1-3) have houses mixed with hotels, resorts, and villas. Sites 13, 15, 17, and 20 (Kertajaya Sumur, Bumi Waras, Wayurang 2, and Kunjir) have high-density housing. Sites 3, 6, 7, and 16 (Sukarame, Mekarsari, Tanjungjaya 1, and Wayurang 1) have agricultural land. Site 14 is a protected national park with limited access. Although this site has no residents, it is very important to review it because it includes the only Javan rhino (*Rhinoceros sondaicus*) habitat in the world. The Javan rhino is one of the most threatened mammals on earth, with a population of less

than 100. The distribution of the rhino indicates that tsunamis are a significant risk to the species in the area (Setiawan et al., 2018).

Each site has a different beach profile. Most sites are natural beaches. Sites 2, 4, 8, 9, and 10 (Pasauran, Pejamben, and Tanjunglesung 1-3) have coastal structures (e.g., sea walls) and sites 5, 17, and 20 (Sukamaju, Wayurang 2, and Kunjir) have
5 revetments.

Figure 1: Locations of field surveys. Sunda Strait lies between Java Island and Sumatra Island in Indonesia. Site numbers are followed by site names. Numbers in brackets indicate inundation distances and run-up heights in meters, respectively

Table 1

Field survey sites and measurements

3 Method

Measurements of run-up and inundation were conducted using conservative **terrestrial** surveying methods with optical and laser devices (e.g., total stations, handheld GPS devices, and laser distance meters). We measured run-up and inundation based on coastline at the time of survey. Run-up were corrected to calculate heights above sea level because the tide level at the time of actual tsunami was different from tidal level at the time of surveys. We use WXTide software version 4.7 for correcting
20 elevation. Elevation values of each survey site were corrected with the nearest tidal gauge available. **Elevation values of each survey site were corrected with the nearest tidal gauge available. We used 3 station in Ciwandan, Labuhan and Teluk Betung, for corrections.** The maximum run-up and inundation limits are based on remaining tsunami trail marks at measurement locations. The tracks were in the form of debris, fallen trees, plants that change color, and damage to buildings. The observed damage to buildings and structures was caused by the tsunami because there were no other causes, such as the earthquake sand
25 liquefaction in the 2018 Sulawesi tsunami (Widiyanto et al., 2019). In addition, information regarding inundation limits and highest run-up was also obtained from eyewitnesses. IOC Manuals and Guides No. 37 (1998 and 2014) and field survey reports (Maramai and Tinti 1997; Farreras 2000; Matsutomiet al. 2001; Fritz and Okal 2008) were used as guidelines for the implementation of this field survey.

Sediment samples were collected from selected points at measurement locations that could be in the swash zone, nearshore, berm, or deposit areas (Table 2 and Fig. 2). The measurement of deposit thickness in sandy sheets was carried out by digging a number of shallow holes. The measured thickness was considered to be near the maximum thickness. This method was qualitative and subjective because tsunami deposits are discontinuous, sporadic, and scattered over a flooded area. Sand sheets deposited on land vary greatly due to the influence of sedimentary sources and topography. A pit was made at each selected point to observe layers suspected to have been produced by the tsunami. We took only one sample at each pit for laboratory
35 testing and did not take vertical samples at intervals of 1 cm, as done by some researchers (Gelfenbaum and Jaffe 2003; Hawkes et al. 2007; Srinivasalu et al. 2007; Srisutam and Wagner 2010), because a detailed analysis was not our focus, particularly the number of tsunami waves and the vertical variation of sediment. The grain size of the samples obtained from the field was tested using ASTM standard sieve analysis. In addition, we investigated boulder movement at four sites.

Figure 2: Aerial photographs from Google Earth of transects including highest run-up point and deposit pit.

4 Run-up

The run-up was measured by determining the height difference between the highest point of sea water rise onto land and the coastline. Run-up is influenced by the characteristics of the ground surface and slope. The measurement results from our field surveys show that run-up ranged from 1 to 9 m (Table 1 and Fig. 1). The values in the table and figure has been corrected for tide to obtain elevation from sea level at time of tsunami. A run-up height of about 1 m was found in many locations, at which no damage was found. The highest run-up was found at the Tanjung Jaya 2, Cagar Alam, and Kunjir sites, with heights of 9.2, 7.8, and 7.7 m respectively. Site Tanjungjaya 2 is located in Cipenyu Beach. Muhari et al. (2019) reported maximum run-up height of 13 m in area around Tanjungjaya/Cipenyu Beach as well. This value is significant different with our maximum run-up since we measure in flat valley part of Cipenyu Beach while Muhari et al. measured in hilly coast of Cipenyu Beach. The Cagar Alam (sanctuary) site is part of the Ujung Kulon National Park. This site has a flat topography and a dense forest. The guard post and water police office were completely destroyed by the tsunami. The Kunjir site, which is densely inhabited, had the second most victims after the Sumur site. This site is located on Sumatra Island about 38 km from the tsunami source. The Tanjung Jaya 2 site is a private resort with many tourists. The topography is relatively flat but suddenly rises at a distance of about 250 m from the coastline due to a long hill. A large boulder moved by the tsunami was found at this site.

Figure3: Positions of deposit pits and deposit limit compared to run-up elevation.

Our surveyed run-up heights are compared with published tide gauge records of Heidarzadeh et al. (2020). Three tide gauges from the article (Ciwandan, Marina Jambu and Panjang) are used. Maximum amplitudes at Ciwandan, Marina Jambu, and Panjang are 1.15 m, 2.8 m, and 1.25 m respectively. Ciwandan tide gauge is used to evaluate run-up heights at site Karangsuruga, Pasauran, Sukarame and Pejamben. Marina Jambu tide gauge is used to evaluate run-up heights at sites Sukamaju, Karangsari, Tanjungjaya 1, Tanjunglesung (1,2,3), Tanjungjaya 2, Banyuasih, Kertajaya Sumur, Cagar Alam. Besides, Panjang tide gauge is used to evaluate sites of Bumiwaras, Wayurang 1, Wayurang 2, Kotaguring, Sukaraja, and Kunjir. It is indicated that averaged run-up heights of each site associated with the tide gauge are 4 times, 1.15 times, and 3.1 times larger than maximum amplitude at the Ciwandan, Marina Jambu, and Panjang respectively. The sites are relatively far from the tide gauge.

5 Inundation

The distance from the run-up point to the coastline is defined as the inundation distance (IOC Manuals and Guides No. 37, 2014). This distance can be easily obtained using a distance measurement instrument or GPS. We used total station for this purpose. The coastlines elevation in our survey were corrected with tide elevation of several tide gauge in Sunda Strait. The results of our field measurements show that the inundation distance ranged from 10 to 290 m (Table 1 and Fig. 1). The wave with an inundation distance of 10 m and a run-up of 1 m at site 15 (Bumi Waras) was not felt by the population. This site was chosen to represent the area of Bandarlampung City, which is the capital of Lampung Province. This city has a population of 1 million (2018) and must thus develop tsunami mitigation strategies. The longest inundation distance was found at site 14 (292.2 m), in the sanctuary, which also had the high run-up. At this site, measurements were made near the mouth of a small river. Long inundation distances may be caused by relatively flat topography with relatively few obstacles. Tsunami may also travel faster through a stream channel. A relatively long inundation (284.2 m) was also found at Tanjungjaya 2, a site with the highest run-up. This site is in the form of a valley plain with a small stream. Slope in the valley is relatively flat and suddenly changing steeply in hilly areas within 250-300 m from coastline. The run-up point we recorded is located on the slope change from mild to steep. These mild and steep areas have slopes of approximately 0.025 and 0.06, respectively. Local people call this area as Cipenyu Beach. This is a sandy beach flanked by cliffs or hilly beaches. Fortunately, not many people live around this site other than at a resort complex, which suffered severe damage.

Figure 4: Positions of deposit pits and deposit limit compared to inundation distance.

6 Tsunami Wave Direction

The tsunami spread out from its source on the Anak Krakatau volcano to the beaches at the edge of Sunda Strait. To determine the direction of the tsunami that arrived at the beach, we obtained information from eyewitnesses. The tsunami hit at night and thus its arrival was difficult to see. Fortunately, it hit during a full moon period, so that there was some light. In addition to eyewitness accounts, we obtained evidence in the field related to the direction of the tsunami propagation. The evidence was in the form of fallen tree trunks, sloping vegetation and shrubs, damaged buildings, and building components carried away by the flow (Fig. 5).

Figure 5: Evidence of tsunami direction. Arrows show the direction of tsunami flow on the ground surfaces.

Our survey results show that the direction of the tsunami propagation was radial from the source (Fig. 6). The tsunami traveled east on the coast between Anyer and Labuhan (sites 1-6). In the vicinity of Tanjunglesung (sites 7-13), the tsunami was directed to the southeast, and in part of Ujung Kulon National Park (Site 14), the tsunami was directed southward. The tsunami was directed to the North and slightly to the northeast on Sumatra Island (sites 15-19). The westward tsunami toward the Tanggamus area was relatively small and insignificant. We did not include this area in the survey. The smaller magnitude of the tsunami to the west is likely due to obstruction by the island of Sertung and bathymetry factors. The Anak Krakatau mountain avalanche had a southwest direction, but the tsunami in this direction had no impact on human life because it leads to the open sea (the Indian Ocean), with increasing depth from the tsunami source. Tsunami wave direction from North arrived in coastal area is given in Table 1 for the field survey sites. The direction ranges from 25° to 350° from North that it indicates radially propagation of the tsunami wave.

Figure 6: Direction of tsunami propagation, the tsunami spread radially from its source.

7 Sediment Characteristics

7.1 Tsunami Deposits

Prehistoric (paleo-) tsunamis have been identified from sediment deposits in several studies (Atwater 1992; Dawson and Shi 2000; Peters, Jaffe and Gelfenbaum 2007). Sediment deposits can be used to explain and reconstruct significant tsunami events (Dawson *et al.* 1995; Van Den Bergh *et al.* 2003). The present study attempts to describe the impact of a recent tsunami on sediment movement around the coastal area. The tsunami carried sediment from the coast inland. However, not all sites that we measured had significant sediment deposits. Only places with a sufficient source of material had clearly observable sediment deposits (Fig. 4). The survey sites used for sediment samples are shown in Fig. 2. Sediment deposits generally do not spread evenly and continuously but are separated at certain locations, which allow it to settle. Topography controls sediment deposits; for instance, there are more sediment deposits at ground surface depressions.

Figure 4: Tsunami sediment deposit, test pits were made to measure the deposit thickness.

The best location for the observation of tsunami sediment is about 50-200 m inland from the coastline (Srisutam and Wagner, 2010) or about 50-400 m inland (Moore *et al.*, 2006), as used for the 2004 Sumatra-Andaman tsunami. In this study, the 12

deposit pits were 15-200 m (average: 93 m) from the shoreline. Four deposit pits were less than 50 m from the shoreline (Figure 6). Three of them were at sites 1, 2, and 7, respectively, due to the short inundation and beach scarp. Another was at site 13 (Kertajaya Sumur), where high-density housing blocked the sediment transport and created a deposit at short distance from the shoreline.

5 The interpretation of tsunami magnitude, especially run-up and inundation based on tsunami deposits, is challenging (Dawson and Shi 2000). However, the relationship between deposits and run-up or inundation is still not convincing because of the high variability of tsunami deposits in terms of thickness and location. Soulsby et al. (2007) proposed a mathematical model for reconstructing tsunami run-up from sedimentary characteristics. The run-up distance for sediment is related to the run-up distance for water as:

$$10 \quad R_s = \frac{R_w}{1+\alpha\gamma} \quad (1)$$

where R_s is the maximum distance inland for sediment deposition, R_w is the run-up limit for water, α is as shown in Eq. 2, and γ is a comparison factor between uprush time and total uprush plus backwash time.

$$\alpha = \frac{w_s T}{H} \quad (2)$$

15 where w_s is the settling velocity, T is a period from the time of first wetting to final drying of inundated ground, and H is the tsunami height. Fig. 7 shows the distance of measured sediment deposition and water run-up compared to the distance of theoretical sediment deposition calculated using Eq. 1 and Eq. 2, the results are in good agreement. However, Sukarame, Tanjungjaya 1 and Cagar Alam do not fit well. The three location have morphological conditions may not ideal for applying the theoretical approach. Sukarame has beach scarp and tsunami flows across a stream around 90 m from coastline. Tanjungjaya 1 has also beach scarp and there is a sea wall, although not so high, that may block the sediment movement. Eventhough
20 Tanjungjaya 1 has abundant material, low amplitude tsunami caused a few sand transport. Cagar Alam has a relative bigger stream than Sukarame. In addition, Cagar Alam has dense vegetation since it is a national park. The distance of area with significant sediment deposits caused by the tsunami from the coast varied in the range of 15-200 m (average: 93 m) from the shoreline or 40%-90% (average: 67%) of the inundation distance.

The sediment samples were tested for gradations in the laboratory. The results for each site are shown in Fig. 8. The sediment
25 in the deposit areas on land is generally finer than at the sources at the beach (nearshore or swash zone). The characteristics of the sediment are discussed in Section 7.3. The sediment deposition thickness varied greatly from one point to another at the survey sites. We chose a test pit with significant thickness for sampling. The thickness was likely near the maximum sediment thickness in the area.

30

7.2 Boulder Movement

Coastal boulder accumulation is usually associated with high-energy events (tsunamis, hurricanes, or powerful storms). A characteristic of many tsunamis is their ability to deposit boulders across the coastal zone (Dawson and Shi, 2000). Extreme
35 storms also have the ability to deposit boulders (Morton, Gelfenbaum and Jaffe 2007; Richmond *et al.* 2010). The interpretation of boulders is difficult along coasts where both storms and tsunamis have occurred. We identified boulders moved by a tsunami wave and run-up at three survey sites based on information from eyewitnesses. Eyewitnesses said that these boulders were in new positions after the tsunami. In addition, from the physical criteria given by Morton et al. (2007) and Paris et al. (2010), it was most likely that the boulders were moved by the tsunami. One of criteria by Morton et al. (2007) we found in this site is a
40 relatively thin (average < 25 cm) bed composed of normally graded sand consisting of a single structureless bed or a bed with only a few thin layers. Sediment thickness around the boulder is very thin. Paris et al. (2010) reported regarding boulder and fine sediment transport and deposition by the 2004 tsunami that most of the sediments deposited on land came from offshore,

from fine sands to coral boulders, and with very high values of shear velocity (>30 cm/s). The boulder we found came from nearshore and a part of the boulder was submerged. We estimate that high shear velocity should occur to transport it. It was most possible by 22 December 2018 tsunami. At about the time of the tsunami event, a tropical cyclone called Kenanga formed in the Indian Ocean about 1400 km from Sunda Strait. Kenanga had a speed of 75 km/h and was active from December 15 to 18, 2018 (Prabowo, 2018). The influence of this cyclone was weak in the coastal zone, and thus it was unlikely to have moved the boulders.

The largest boulder, measuring 2.7 m in diameter (10.4 tons), was found at site 11 (Tanjungjaya 2), as shown in Fig. 7a. This boulder moved from its original point in the swash zone to 81 m inland. Other smaller stones were scattered around it. In Tanjunglesung (sites 8, 9, and 10), pebbles, cobbles, and small boulders (25-50 cm) were scattered up to 40 m from the coastline. At site 4, the seawall built to protect a hotel and villas was partly destroyed and moved ashore. A seawall chunk, measuring 1 m \times 1 m \times 4.2 m (9.5 tons), made from rubble mound and mortar moved as far as 30 m from its place of origin (Fig. 7b). Other smaller chunks were also moved.

Figure 7: (a) Boulder that moved around 82 m inland and (b) an element of seawall that moved around 30 m inland.

15

The characteristics of the boulders moved by a tsunami can be used to estimate the associated flow velocities. For instance, the 2004 tsunami had flow velocities of 3-13 m/s. This tsunami drove a 7.7-ton calcareous boulder 200 m and an 11-ton coral boulder as far as 900 m (Paris et al., 2010). The velocity was calculated as:

$$u = \sqrt{\left(\frac{2\mu mg}{C_d A_n \rho_w}\right)} \quad (3)$$

20 where μ is the friction coefficient, m is the boulder mass (kg), g is the gravitational acceleration, C_d is the drag coefficient, A_n is the area of the boulder projected normal to the flow (m^2), and ρ_w is the density of sea water (kg/m^3). The velocities were calculated from Equation 3 to be $u \geq 4.5$ m/s and $u \geq 4.0$ m/s for the 10.4-ton (Fig. 7a) and 9.4-ton (Fig. 7b) boulders, respectively.

25 7.3 Sand Size Statistics

The results of sieve analysis, namely sand grain size distributions, are shown as a cumulative distribution curve of sand grain size. Fig. 8 shows the cumulative distribution curve for 12 sites. From the curve, various diameter values were determined, including d_{95} , d_{84} , d_{50} , d_{16} , and d_5 . From these diameters, other statistics can be determined, namely the mean, standard deviation, skewness, and kurtosis (Table 2). The mean can be used for grain size classification. The standard deviation is a measure of range that shows the uniformity of a sand sample. A perfectly sorted sample will have sand of the same diameter, whereas poorly sorted sand will have a wide size range. Beach sand size distributions with a standard deviation of ≤ 0.5 are considered well sorted, and those with a standard deviation of ≥ 1 are assumed to be poorly sorted. Skewness occurs when the sand size distribution is not symmetrical. A negative skewness value indicates that the distribution is tending to the value of small phi (large grain size). Kurtosis determines the peakedness of the size distribution. The normal distribution has a kurtosis value of 0.65. If the distribution is more diffuse and wider than the normal distribution, the kurtosis value will be less than 0.65 (Dean and Dalrymple, 2004).

35

Figure 8: Sediment grain size results from sieve analysis for various sites.

40 From our results, the mean values show that medium and coarse were the dominant types of sand in the sample. Very coarse sand, granular sand, and pebbles were found at the Tanjungjaya 2 and Sukarame sites. Fine and very fine sand was also identified at several sites. The range of grain sizes found in the study area depends on the available source material. Wentworth

classification was used to assess the grain size. All samples had negative standard deviations, indicating that they had well sorted distributions.

Table 2 Sediment statistics and characteristics

5

7 of the 10 samples taken from the swash zone had negative skewness, which indicated a large phi value and an erosive tendency in the zone. The numbers of samples with positive and negative skewness were similar (7 and 6, respectively). Some deposit samples were taken at a distance of less than 50 m from the coastline, which may still be an erosive environment.

The kurtosis of the tsunami sediment indicates that grain size distributions were flat to peaked distribution. Generally, the major sources of tsunami sediment are swash zones and berm/dune zone sands, where coarse to medium sands are dominant. A minor source of tsunami sediment is the shoreface, where fine to very fine sands are dominant. However, for a coastal area where the shoreface slope is mild, the major source of tsunami sediment is the shoreface. Table 2 provides kurtosis values from which distribution of sediment range from very platykurtic to very leptokurtic.

8 Conclusion

15 We selected 20 sites on Java Island and Sumatra Island to observe the impact of the December 2018 tsunami, which was caused by a mass movement of an Anak Krakatau volcano flank. The survey results revealed that the run-up height ranged from 1 to 9 m, the inundation distance was 10 to 300 m, and the direction of the tsunami was between 25° and 350°. The highest run-up (9.2 m) was found at site Tanjungjaya 2. The longest inundation distance (292 m) was found and site Cagar Alam which contains a forest area, part of a national park, and a UNESCO heritage site. Sediment samples were taken from
20 27 points in tsunami deposits with a sediment thickness of 1.5-12 cm. The distance of area with significant sediment deposits caused by the tsunami from the coast varied in the range of 15-200 m (average: 93 m) from the shoreline or 40%-90% (average: 67%) of the inundation distance. The elevations of the significant sediment deposits reached 60%-90% (average: 81%) of the run-up elevation. Sediment material larger than coarse sand (granular sand, pebbles, cobbles, and boulders) was found at several locations. The largest boulder has a diameter of 2.7 m and a weight of 10.4 tons. From the boulder movement, the
25 tsunami velocity at the ground surface is estimated to be more than 4.5 m/s. Sand size statistics are also given in this report. The sediment grain size ranged from very fine sand to boulders, with medium sand (diameter: 0.25-0.5 mm) and coarse sand (diameter: 0.5 -1.0 mm) being dominant. All sediment samples tested in the laboratory has a well sorted distribution, indicating that the grain sizes were relatively uniform.

Acknowledgment

30 The authors would like to thank the Geomatics Laboratory and the Soil Mechanics Laboratory at the Civil Engineering Department, Universitas Jenderal Soedirman, Purwokerto, Indonesia. We would also like to thank Ujung Kulon National Park and Tanjung Lesung Special Economic Zone for conducting surveys in their areas. We are grateful to Mr. Sumantri from Tanjunglesung Special Economic Zone and Mr. Budi Prasetyo from Carita Resort for accompanying the tsunami impact review and providing detailed chronological information on the tsunami, especially in Tanjunglesung and Carita Beach, respectively.
35 We appreciate Ms. Sanidhya Nika Purnomo for discussion on geographical information.

Financial Support

This study was funded by the Ministry of Science and Technology, Taiwan, under grant MOST 108-2221-E-006-087 and MOST 109-2217-E-006-002-MY3.

40

References

- Atwater, B. F.: Geologic evidence for earthquakes during the past 2000 years along the Copalis River, southern coastal Washington, *J. Geophys. Res. Solid Earth*, 97(B2), 1901–1919, doi:10.1029/91jb02346, 1992.
- BPS-Statistics of Banten Province: Banten Province in Figures 2019, Serang, 2019.
- 5 BPS-Statistics Indonesia: Statistical Yearbook of Indonesia 2019, Jakarta, 2019.
- BPS-Statistics of Lampung Province: Lampung Province in Figures 2019, Bandar Lampung, 2019.
- Camus, G., Diament, M., Gloaguen, M., Provost, A. and Vincent, P.: Emplacement of a Debris Avalanche during the 1883 eruption of Krakatau (Sunda Straits, Indonesia), *GeoJournal*, 28(2), 123–128, doi:10.1007/BF00177224, 1992.
- Dawson, A. G. and Shi, S.: Tsunami Deposits, *Pure appl. Geophys*, 157, 875–897, 2000.
- 10 Dawson, A. G., Hindson, R., Andrade, C., Freitas, C. and Parish, R.: Tsunami sedimentation associated with the Lisbon earthquake of 1 November AD 1755 Boca do Rio, Algarve, Portugal, *The Holocene*, 5(2), 209–215, 1995.
- Dean, R. G. and Dalrymple, R. A.: *Coastal Processes with Engineering Application*, 1st ed., Cambridge University Press, Cambridge., 2004.
- Dirjen Perhubungan Darat: *Perhubungan Darat dalam Angka 2018*, Jakarta, 2019
- 15 Farreras, S. F.: Post-tsunami field survey procedures: An outline, *Nat. Hazards*, 21(2–3), 207–214, doi:10.1023/A:1008049228148, 2000.
- Fritz, H. M. and Okal, E. A.: Socotra Island, Yemen: Field survey of the 2004 Indian Ocean tsunami, *Nat. Hazards*, 46(1), 107–117, doi:10.1007/s11069-007-9185-3, 2008.
- Gelfenbaum, G. and Jaffe, B.: Erosion and sedimentation from the 17 July, 1998 Papua New Guinea tsunami, *Pure Appl. Geophys.*, doi:10.1007/s00024-003-2416-y, 2003.
- 20 Giachetti, T., Paris, R., Kelfoun, K. and Ontowirjo, B.: Tsunami hazard related to a flank collapse of Anak Krakatau Volcano, Sunda Strait, Indonesia, *Geol. Soc. London, Spec. Publ.*, 361(1), 79–90, doi:10.1144/sp361.7, 2012.
- Hawkes, A. D., Bird, M., Cowie, S., Grundy-Warr, C., Horton, B. P., Shau Hwai, A. T., Law, L., Macgregor, C., Nott, J., Ong, J. E., Rigg, J., Robinson, R., Tan-Mullins, M., Sa, T. T., Yasin, Z. and Aik, L. W.: Sediments deposited by the 2004 Indian Ocean Tsunami along the Malaysia–Thailand Peninsula, *Mar. Geol.*, doi:10.1016/j.margeo.2007.02.017, 2007.
- 25 Heidarzadeh, M., Ishibe, T., Sandanbata, O., Muhari, A., Wijanarto, A.B. (2020). Numerical modeling of the subaerial landslide source of the 22 December 2018 Anak Krakatoa volcanic tsunami, Indonesia. *Ocean Engineering*, 195, <https://doi.org/10.1016/j.oceaneng.2019.106733>.
- IOC Manuals and Guides No. 37: *International Tsunami Survey Team (ITST) Post-Tsunami Survey Field Guide*, 2nd ed., edited by D. Dominey-Howes, L. Dengler, J. Cunnien, and T. Aarup, the United Nations Educational, Scientific and Cultural Organization, Paris., 2014.
- 30 Kasbani: *Pers Rilis Aktivitas Gunung Anak Krakatau*, 28 Desember 2018, 2018.
- Maeno, F. and Imamura, F.: Tsunami generation by a rapid entrance of pyroclastic flow into the sea during the 1883 Krakatau eruption, Indonesia, *J. Geophys. Res. Solid Earth*, 116(9), 1–24, doi:10.1029/2011JB008253, 2011.
- 35 Maramai, A. and Tinti, S.: The 3 June 1994 Java Tsunami: A post-event survey of the coastal effects, *Nat. Hazards*, doi:10.1023/A:1007957224367, 1997.
- Matsutomi, H., Shuto, N., Imamura, F. and Takahashi, T.: Field survey of the 1996 Irian Jaya earthquake Tsunami in Biak Island, *Nat. Hazards*, 24(3), 199–212, doi:10.1023/A:1012042222880, 2001.
- Moore, A., Nishimura, Y., Gelfenbaum, G., Kamataki, T. and Triyono, R.: Sedimentary deposits of the 26 December 2004 tsunami on the northwest coast of Aceh, Indonesia, *Earth Planets Sp.*, 58, 253–258, 2006.
- 40 Morton, R. A., Gelfenbaum, G. and Jaffe, B. E.: Physical criteria for distinguishing sandy tsunami and storm deposits using modern examples, *Sediment. Geol.*, doi:10.1016/j.sedgeo.2007.01.003, 2007.

- Muhari, A., Heidarzadeh, M., Susmoro, H., Nugroho, H.D., Kriswati, E., Supartoyo, Wijanarto, A.B., Imamura, F., Arikawa, T. (2019). The December 2018 Anak Krakatau volcano tsunami as inferred from post-tsunami field surveys and spectral analysis. *Pure and Applied Geophysics*, <https://doi.org/10.1007/s00024-019-02358-2>.
- Paris, R., Fournier, J., Poizot, E., Etienne, S., Morin, J., Lavigne, F. and Wassmer, P.: Boulder and fine sediment transport and deposition by the 2004 tsunami in Lhok Nga (western Banda Aceh, Sumatra, Indonesia): A coupled offshore-onshore model, *Mar. Geol.*, doi:10.1016/j.margeo.2009.10.011, 2010.
- Paris, R., Wassmer, P., Lavigne, F., Belousov, A., Belousova, M., Iskandarsyah, Y., Benbakkar, M., Ontowirjo, B. and Mazzoni, N.: Coupling eruption and tsunami records: The Krakatau 1883 case study, Indonesia, *Bull. Volcanol.*, 76(4), 1–23, doi:10.1007/s00445-014-0814-x, 2014.
- Peters, R., Jaffe, B. and Gelfenbaum, G.: Distribution and sedimentary characteristics of tsunami deposits along the Cascadia margin of western North America, *Sediment. Geol.*, doi:10.1016/j.sedgeo.2007.01.015, 2007.
- Prabowo, M. R.: Siklon Tropis “Kenanga” Tumbuh di Samudra Hindia Selatan Sumatera, bmgk.go.id, 2018.
- Richmond, B. M., Buckley, M., Gelfenbaum, G., Morton, R. A., Watt, S. and Jaffe, B. E.: Recent storm and tsunami coarse-clast deposit characteristics, southeast Hawai‘i, *Mar. Geol.*, doi:10.1016/j.margeo.2010.08.001, 2010.
- Setiawan, R., Gerber, B. D., Rahmat, U. M., Daryan, D., Firdaus, A. Y., Haryono, M., Khairani, K. O., Kurniawan, Y., Long, B., Lyet, A., Muhiban, M., Mahmud, R., Muhtarom, A., Purastuti, E., Ramono, W. S., Subrata, D. and Sunarto, S.: Preventing Global Extinction of the Javan Rhino: Tsunami Risk and Future Conservation Direction, *Conserv. Lett.*, 11(1), doi:10.1111/conl.12366, 2018.
- Soeriaatmadja, W.: Indonesia plans traffic system for busy Sunda Strait, available at <https://www.straitstimes.com/asia/south-asia/indonesia-plans-traffic-system-for-busy-sunda-strait> (last access, 10 January 2020), 2020.
- Srinivasalu, S., Thangadurai, N., Switzer, A. D., Ram Mohan, V. and Ayyamperumal, T.: Erosion and sedimentation in Kalpakkam (N Tamil Nadu, India) from the 26th December 2004 tsunami, *Mar. Geol.*, doi:10.1016/j.margeo.2007.02.003, 2007.
- Srisutam, C. and Wagner, J. F.: Tsunami sediment characteristics at the Thai Andaman Coast, *Pure Appl. Geophys.*, doi:10.1007/s00024-009-0015-2, 2010.
- Van Den Bergh, G. D., Boer, W., DeHaas, H., Van Weering, T. C. E. and Van Wijhe, R.: Shallow marine tsunami deposits in Teluk Banten (NW Java, Indonesia), generated by the 1883 Krakatau eruption, *Mar. Geol.*, 197(1–4), 13–34, doi:10.1016/S0025-3227(03)00088-4, 2003.
- Verbeek, R. D. M.: The Krakatoa Eruption, *Nature*, 10–15, 1884.
- Widiyanto, W., Santoso, P. B., Hsiao, S.-C. and Imananta, R. T.: Post-event Field Survey of 28 September 2018 Sulawesi Earthquake and Tsunami, *Nat. Hazards Earth Syst. Sci. Discuss.*, (September 2018), 1–23, doi:10.5194/nhess-2019-91, 2019.
- Yokoyama, I.: A scenario of the 1883 Krakatau tsunami, *J. Volcanol. Geotherm. Res.*, 34(1–2), 123–132, doi:10.1016/0377-0273(87)90097-7, 1987.

35

40

Table 1 Field survey sites and measurements

Site	Site name	Measurement time	Coordinates		Inundation distance (m)	Uncorrected Run-up height (m)	Corrected Run-up height (m)	Tsunami direction from North (°)	Sediment sample numbers
			Long. (°)	Lat. (°)					
1	Karangsuraga	25 Jan 2019	-6.148434	105.854718	84.00	4.7	4.72	82	S-01, S-02
2	Pasauran	25 Jan 2019	-6.202289	105.836179	111.00	5.8	5.41	84	S-03, S-04
3	Sukarame	24 Jan 2019	-6.261508	105.830448	204.66	4.1	3.59	93	S-05, S-06, S-07
4	Pejamben	24 Jan 2019	-6.316783	105.831298	200.80	5.0	4.61	105	-
5	Sukamaju	24 Jan 2019	-6.390917	105.825965	125.85	2.2	1.47	110	-
6	Mekarsari	25 Jan 2019	-6.520795	105.758381	123.80	2.3	1.55	115	S-08
7	Tanjungjaya 1	27 Jan 2019	-6.509201	105.673902	60.57	1.1	0.96	210	S-09, S-10
8	Tanjunglesung 1	23 Jan 2019	-6.480980	105.659513	149.54	3.4	3.03	135	S-11, S-12, S-13
9	Tanjunglesung 2	23 Jan 2019	-6.480914	105.654575	202.17	3.6	3.45	128	-
10	Tanjunglesung 3	23 Jan 2019	-6.481270	105.652097	177.06	2.4	2.40	133	S-14, S-15, S-16
11	Tanjungjaya 2	23 Jan 2019	-6.504584	105.642052	284.17	7.0	6.16	120	S-17, S-18, S-19
12	Banyuasih	23 Jan 2019	-6.600539	105.621017	170.30	2.1	1.21	142	-
13	Kertajaya Sumur	26 Jan 2019	-6.656894	105.583253	134.68	5.0	4.25	150	S-20, S-21
14	Cagar Alam	26 Jan 2019	-6.676569	105.378788	292.19	7.8	7.64	180	S-22, S-23, S-24
15	Bumi Waras	28 Jan 2019	-5.459514	105.262263	10.00	1.1	1.21	350	-
16	Wayurang 1	28 Jan 2019	-5.72307	105.582329	181.58	4.2	4.51	30	S-25, S-26, S-27
17	Wayurang 2	28 Jan 2019	-5.745806	105.587961	81.34	4.2	4.45	34	-
18	Kotaguring	28 Jan 2019	-5.800583	105.584414	29.07	2.6	2.81	25	-
19	Sukaraja	28 Jan 2019	-5.833699	105.626956	64.44	2.4	2.56	40	-
20	Kunjir	28 Jan 2019	-5.834768	105.642150	207.13	7.7	7.83	47	-

5

10

Table 2 Sediment statistics and characteristics

Sample	Date (dd/mm/yy)	Time (+8 UTC	Lat. (°S)	Long. (°E)	Village	Subdistrict	Regency	Zone	Deposit thickness (cm)	MedianD ₅₀ (mm)	Φ ₅₀	Mean	Std. Dev.	Skew- ness	Kurto- sis	Remarks
S-01	25/01/19	16:30:38	-6.148187	105.854549	Karangsuraga	Cinangka	Serang	swash zone	-	0.650	0.621	0.883	-1.368	-0.191	-0.864	coarse sand, well sorted, very platykurtic
S-02	25/01/19	16:45:44	-6.148195	105.854774	Karangsuraga	Cinangka	Serang	deposit	12	0.330	1.599	1.698	-0.698	-0.141	0.504	medium sand, well sorted, very platykurtic
S-03	25/01/19	15:02:22	-6.202145	105.835194	Pasauran	Cinangka	Serang	swash zone	-	0.200	2.322	0.007	-2.177	1.063	0.536	coarse sand, well sorted, very platykurtic
S-04	25/01/19	15:19:01	-6.201856	105.835437	Pasauran	Cinangka	Serang	deposit	3	0.500	1.000	0.652	-1.237	0.281	0.603	coarse sand, well sorted, very platykurtic
S-05	24/01/19	16:44:32	-6.260923	105.828634	Sukarame	Labuhan	Pandeglang	nearshore	-	3.000	-1.585	-1.243	-1.757	-0.195	0.463	granular, well sorted, very platykurtic
S-06	24/01/19	16:49:13	-6.261013	105.828977	Sukarame	Labuhan	Pandeglang	swash zone	-	0.500	1.000	0.921	-0.769	0.103	0.599	coarse sand, well sorted, very platykurtic
S-07	24/01/19	16:54:01	-6.261021	105.829628	Sukarame	Labuhan	Pandeglang	deposit	6.3	0.500	1.000	0.268	-1.368	0.461	0.579	coarse sand, well sorted, very platykurtic
S-08	25/01/19	18:54:59	-6.520795	105.758381	Mekarsari	Panimbang	Pandeglang	deposit	12.7	0.330	1.599	1.656	-0.740	-0.076	0.497	medium sand, well sorted, very platykurtic
S-09	27/01/19	08:34:50	-6.509219	105.674029	Tanjungjaya 1	Panimbang	Pandeglang	swash zone	-	0.240	2.059	1.994	-0.743	0.087	1.516	medium sand, well sorted, very leptokurtic
S-10	27/01/19	08:35:35	-6.509201	105.672903	Tanjungjaya 1	Panimbang	Pandeglang	deposit	2	0.650	0.621	0.128	-1.561	0.316	0.550	coarse sand, well sorted, very platykurtic
S-11	23/01/19	12:22:32	-6.479796	105.658553	Tanjunglesung 1	Panimbang	Pandeglang	swash zone	-	0.220	2.184	2.266	-0.792	-0.103	0.790	fine sand, well sorted, platykurtic
S-12	23/01/19	12:15:53	-6.480013	105.658580	Tanjunglesung 1	Panimbang	Pandeglang	deposit	3	0.170	2.556	2.791	-1.005	-0.233	0.715	fine sand, well sorted, platykurtic
S-13	23/01/19	12:32:23	-6.480799	105.659432	Tanjunglesung 1	Panimbang	Pandeglang	deposit	1.5	0.260	1.943	1.808	-0.749	0.181	1.730	medium sand, well sorted, very leptokurtic
S-14	23/01/19	10:52:19	-6.480284	105.652178	Tanjunglesung 3	Panimbang	Pandeglang	swash zone	-	0.400	1.322	1.630	-0.844	-0.365	0.722	medium sand, well sorted, very leptokurtic
S-15	23/01/19	11:04:00	-6.480438	105.652278	Tanjunglesung 3	Panimbang	Pandeglang	deposit	6.8	0.410	1.286	1.117	-0.883	0.192	1.936	medium sand, well sorted, very leptokurtic
S-16	23/01/19	11:53:24	-6.481134	105.652333	Tanjunglesung	Panimbang	Pandeglang	deposit	3.2	0.380	1.396	1.619	-0.703	-0.317	2.008	medium sand, well sorted, very leptokurtic
S-17	23/01/19	14:28:44	-6.503221	105.639871	Tanjungjaya 2	Panimbang	Pandeglang	nearshore	-	4.200	-2.070	-2.276	-1.074	0.191	0.365	pebble, well sorted, very platykurtic
S-18	23/01/19	14:38:08	-6.502949	105.640477	Tanjungjaya 2	Panimbang	Pandeglang	swash zone	-	1.200	-0.263	-0.026	-1.460	-0.163	0.332	very coarse sand, well sorted, very platykurtic
S-19	23/01/19	14:51:05	-6.504377	105.641338	Tanjungjaya 2	Panimbang	Pandeglang	deposit	-	0.380	1.396	1.429	-0.893	-0.037	0.588	medium sand, well sorted, very platykurtic
S-20	26/01/19	18:40:59	-6.655898	105.583705	Kertajaya	Sumur	Pandeglang	swash zone	-	0.950	0.074	0.465	-1.272	-0.037	0.778	coarse sand, well sorted, platykurtic
S-21	26/01/19	14:42:08	-6.656034	105.583687	Kertajaya	Sumur	Pandeglang	deposit	2	0.220	2.184	1.826	-0.911	0.393	1.131	medium sand, well sorted, leptokurtic
S-22	26/01/19	12:27:00	-6.673185	105.379727	Cagar Alam	Sumur	Pandeglang	nearshore	-	0.220	2.184	1.800	-0.937	0.410	1.654	medium sand, well sorted, very leptokurtic
S-23	26/01/19	13:14:17	-6.674877	105.379122	Cagar Alam	Sumur	Pandeglang	swash zone	-	0.380	1.396	1.494	-0.828	-0.119	1.071	medium sand, well sorted, mesokurtic
S-24	26/01/19	14:03:24	-6.675483	105.378968	Cagar alam	Sumur	Pandeglang	deposit	7.5	0.120	3.059	3.020	-0.624	0.063	0.861	very fine sand, well sorted, platykurtic
S-25	28/01/19	14:04:46	-5.724157	105.581636	Wayurang 1	Kalianda	S. Lampung	nearshore	-	0.190	2.396	2.370	-0.814	0.031	0.697	fine sand, well sorted, platykurtic
S-26	28/01/19	13:48:51	-5.723089	105.581996	Wayurang 1	Kalianda	S. Lampung	swash zone	-	0.190	2.396	2.398	-0.660	-0.003	0.995	fine sand, well sorted, mesokurtic
S-27	28/01/19	14:04:46	-5.724157	105.581636	Wayurang 1	Kalianda	S. Lampung	deposit	12.3	0.170	2.556	2.959	-0.930	-1.718	-2.248	coarse sand, well sorted, very platykurtic

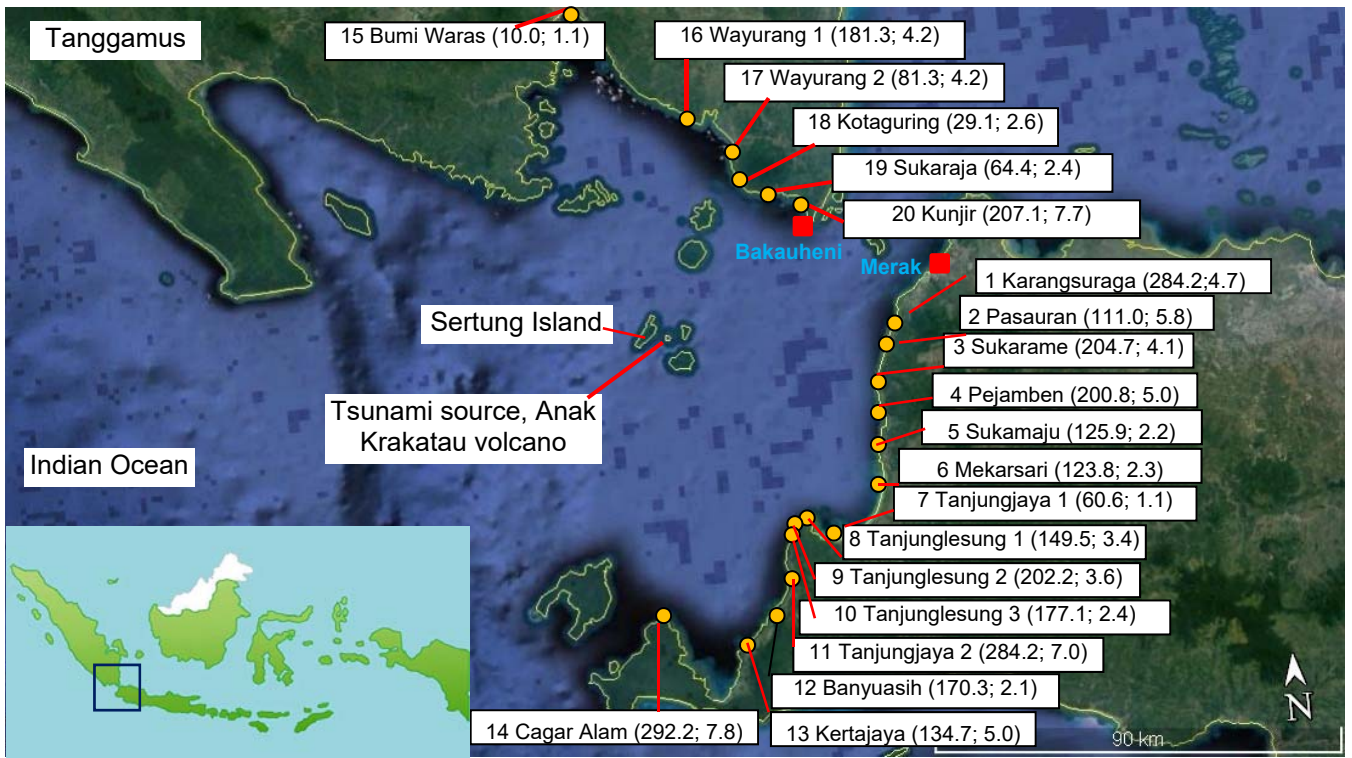
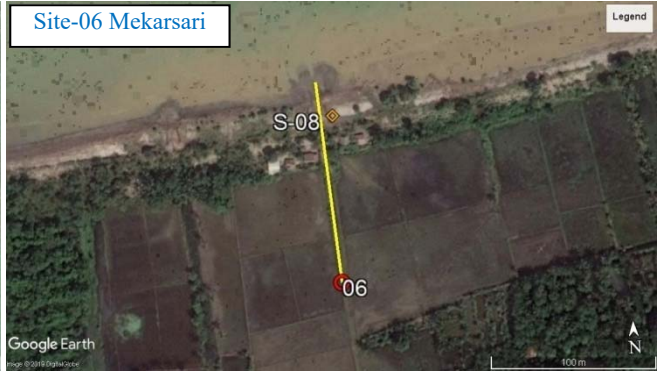


Figure1: Locations of field surveys. Sunda Strait lies between Java Island and Sumatra Island in Indonesia. Site numbers are followed by site names. Numbers in brackets indicate inundation distances and run-up heights in meters, respectively.

5

10

15



5



	Highest point of run-up, Nearby number is survey site numbers
	Sediment test pit
S-xx	Sediment sample number
	transect

5 Figure 2: Aerial photographs from Google Earth of transects including highest run-up point and deposit pit.

10

15

20

25

5



10 Figure 3: Evidence of tsunami direction. Arrows show the direction of tsunami flow on the ground surfaces.

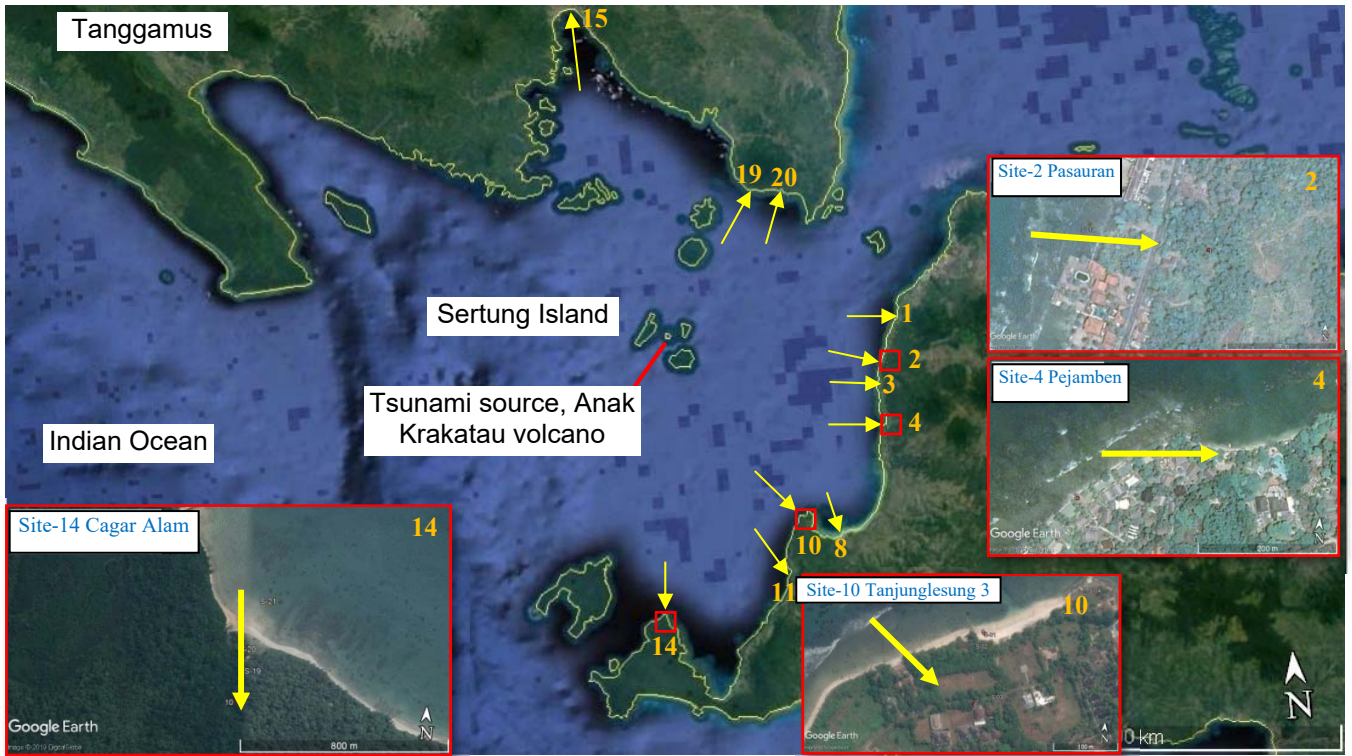


Figure 4: Direction of tsunami propagation, the tsunami spread radially from its source. Numbers shown are survey site numbers.

5



Figure 5: Tsunami sediment deposit, test pits were made to measure the deposit thickness.

10

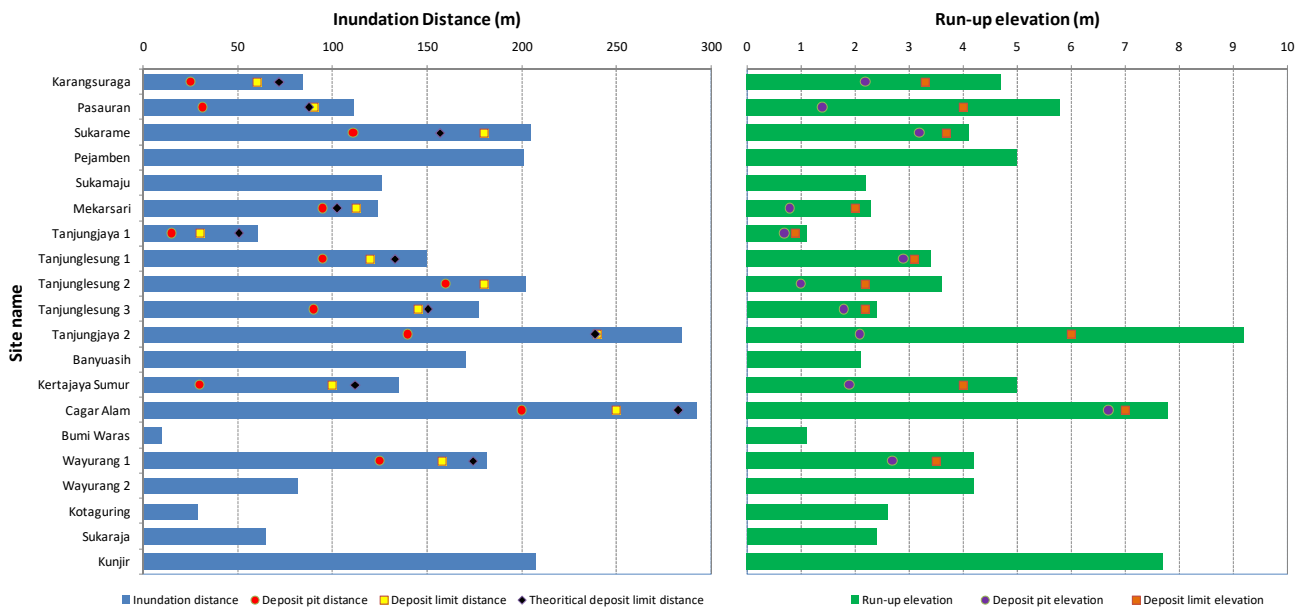


Figure 6: Positions of deposit pits and deposit limit compared to inundation distance and run-up elevation. Theoretical approach for tsunami deposit only available for distance not for elevation.

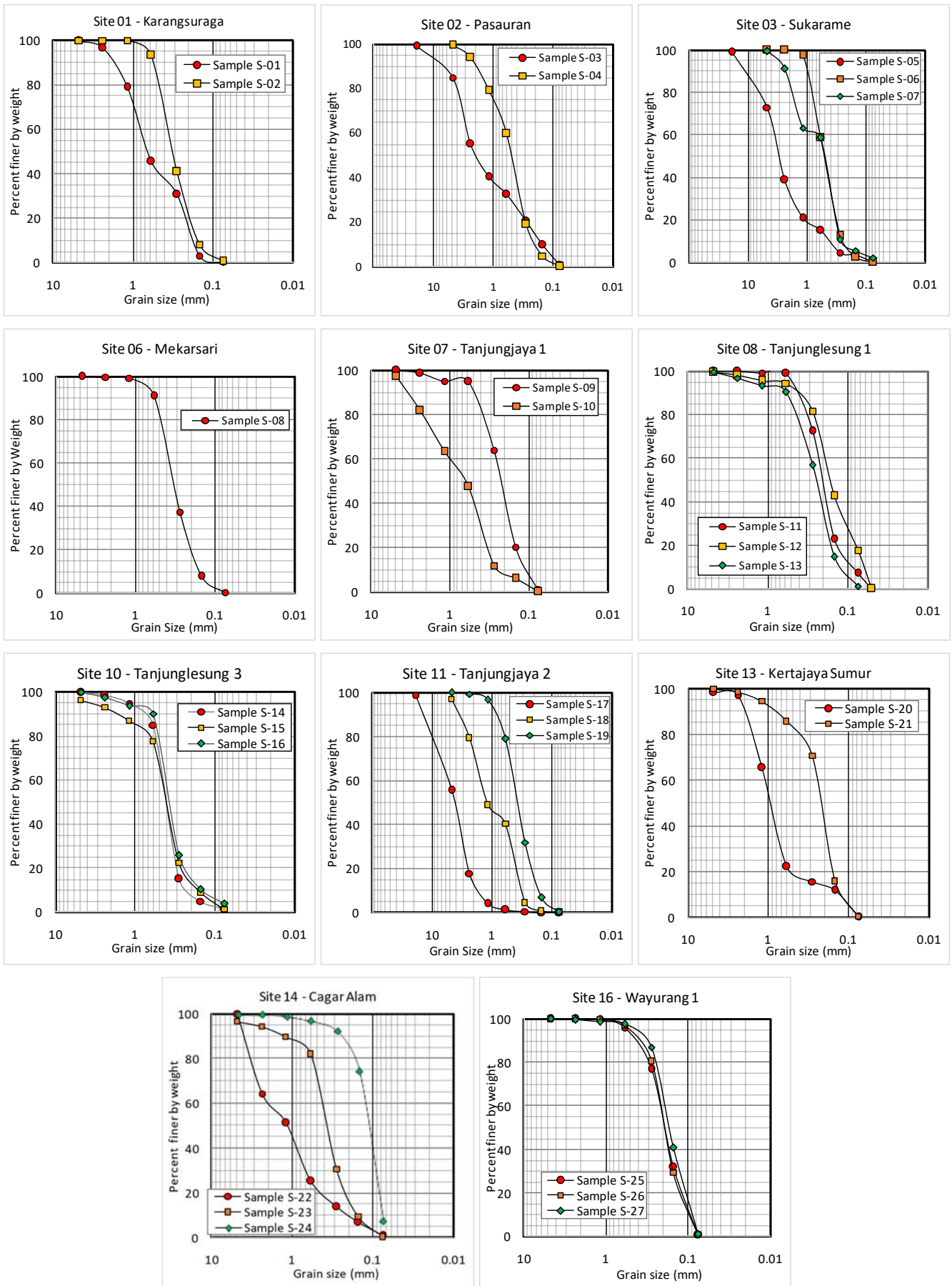
5

10



15

Figure 7: (a) Boulder that moved around 82 m inland in **Tanjungjaya 2** and (b) an element of seawall that moved around 30 m inland in **Pejamben**.



5 Figure 8: Sediment grain size results from sieve analysis for various sites.

Runup, Inundation, and Sediment Characteristics of December 22 2018 Indonesia Sunda Strait Tsunami

Wahyu Widiyanto^{1,2}, Wei-Cheng Lian¹, Shih-Chun Hsiao¹, Purwanto B. Santoso², Rudy T. Imananta³

¹Department of Hydraulic and Ocean Engineering, National Cheng Kung University, Tainan, 701, Taiwan

5 ²Department of Civil Engineering, Universitas Jenderal Soedirman, Purwokerto, 53122, Indonesia

³Meteorological, Climatological and Geophysical Agency (BMKG), Jakarta, 10720, Indonesia

Correspondence to: Shih-Chun Hsiao (schsiao@mail.ncku.edu.tw)

Abstract. A tsunami caused by a flank collapse of the southwest part of the Anak Krakatau volcano occurred on December 22, 2018. The affected area of the tsunami included a coastal area located at the edge of Sunda Strait, Indonesia. To gain an understanding of the tsunami event, field surveys were conducted a month after the incident. The surveys included measurements of runup height, inundation distance, tsunami direction, and sediment characteristics at 20 selected sites. The survey results revealed that the runup height and inundation distance reached 7.8 m and 292.2 m, both was found at Site Cagar Alam, part of Ujung Kulon National Park. Tsunami propagated radially from its source and arrived in coastal zone with direction was between 25° and 350° from North. Sediment samples were collected at 27 points in tsunami deposits with a sediment thickness of 1.5-12 cm. The distance of the sediment deposit area from the coast was 40%-90% of the distance of the inundation caused by the tsunami. The highest elevation of deposits was 60%-90% of the highest runup. Sand sheets were sporadic, highly variable, and highly influenced by topography. Grain sizes in the deposit area were finer than those at their sources. The sizes ranged from fine sand to boulders, with medium sand and coarse sand being dominant. All sediment samples had a well sorted distribution. An assessment of the boulder movements indicates that the tsunami runup had minimum velocities of 4.0-4.5 m/s.

Keywords: tsunami, runup, inundation, sediment, Sunda Strait, Krakatau, field survey

1 Introduction

A tsunami took place in Sunda Strait on December 22, 2018, at 22:00 Western Indonesia Time (+7 UTC). It shocked the local residents because it came without any warning signs, such as earthquake shocks. The source of the tsunami was the Anak Krakatau volcano, a sea mountain in the middle of Sunda Strait. The southwestern slope of the mountain experienced a landslide below the sea surface that resulted in the movement of sea water, which propagated to land in the form of a tsunami wave. When the tsunami reached land, its large energy caused a lot of damage and casualties. Records obtained from the Indonesian National Disaster Management Agency (Indonesian: Badan Nasional Penanggulangan Bencana, BNPB) show 430 deaths, 1015 collapsed houses, and a lot of other damage (e.g., seawalls, revetments, jetties, boats, and cars). The affected areas in Banten Province include Pandeglang and Serang Districts and those in Lampung Province include the regencies of South Lampung, Tanggamus, and Pesawaran.

Sunda Strait is home to the Krakatau (or Krakatoa) volcano. It is famous for the 1883 Krakatau eruption, which caused a 30-m tsunami that led to 36,000 fatalities and affected the Earth's climate and weather for several weeks, as reported by Verbeek (1884). The 1883 eruption of Krakatau and the resulting tsunami have been widely discussed (e.g., Yokoyama 1987; Camus *et al.* 1992; Maeno and Imamura 2011; Paris *et al.* 2014). A young volcano called Anak Krakatau (Child of Krakatau) appeared above sea level in 1929. It grew to 338 m above sea level in September 2018. This very active volcano was the source of the tsunami discussed in the present study.

The generation of the tsunami that occurred on December 22, 2018, in Sunda Strait was triggered by the collapse of a flank in the southwest part of the Anak Krakatau volcano. Satellite imagery shows that the area of the body of the marine volcano that was lost was 64 hectares; the collapsed volume was estimated to be 150-180 million m³ (Kasbani, 2018). As a result of the collapse of some of the volcano's body, the volcano's height decreased from 338 to 110 m above sea level. The tsunami caused by the collapse of the Anak Krakatau flank was investigated by Giachetti et al. (2012). They used a numerical model to simulate an unstable flank collapse in the southwest part of Anak Krakatau. A hypothetical volume of 280 million m³ produces a wave with an initial height of 43 m on Sertung, Panjang, and Rakata islands that then spreads to the beaches in the western part of Java Island, including Merak, Anyer, Carita, Panimbang, and Labuhan, and Sumatra Island, reaching Bandar Lampung City. The actual area affected by the December 22 event is consistent with their model, but different in magnitude due to the use of the worst case scenario in the simulation.

Tsunamis in Sunda Strait are of great concern because the strait is important both locally and globally. It connects the two main islands of Java and Sumatra, whose population accounts for 79% of Indonesia's population. About 6.9 million people live in the coastal area of the strait in Banten Province and Lampung Province. The strait, between Merak and Bakauheni, is the busiest inter-island crossing in Indonesia, with more than 50,000 passengers/day and more than 20,000 vehicles/day. The strait is also an international route for large ships. It is the second-most crowded waterway after Malacca Strait, with 70,000 vessels a year passing it. There are three industrial regions at the edge of the strait, namely Cilegon, Serang, and Tanggamus. There is also a special economic zone in this region, namely Tanjung Lesung. The beaches in the strait are a tourist destination. There are two UNESCO world heritage sites across from each other; one at the western tip of Java Island (Ujung Kulon National Park) and the other at the southern tip of Sumatra Island (Bukit Barisan Selatan National Park). Bandar Lampung, which has a population of 1 million, is the provincial capital and faces the strait directly. Jakarta, the capital of the Republic of Indonesia, is relatively close to the strait.

Post-tsunami field surveys were conducted to obtain data for future mitigation and development activities in the region. The surveys began exactly a month after the tsunami, January 22, and ended on January 28, 2019. Our team included people from Indonesia and Taiwan. We carried out measurements of the runup height and inundation distance of the tsunami. In addition, we also measured flow directions and sediment deposits caused by the tsunami.

2 Study Area

The tsunami has had a serious impact on life in the surrounding area. The affected area covers the coastal area on the western tip of Java Island (Banten Province) and the southern tip of Sumatra Island (Lampung Province). Banten Province covers two districts, namely Serang and Pandeglang. Lampung Province covers South Lampung Regency and the provincial capital of Lampung, namely Bandar Lampung. Post-tsunami field surveys were conducted in these areas. We selected 20 sites for observation and measurement (Table 1 and Fig. 1). These sites are located along 140 km of coast on Java Island and 80 km of coast on Sumatra Island. Sites 13 and 14 were reached by boat because of the difficult land route.

Land use at these sites includes housing, agriculture, tourism, and a national park. Sites 1, 2, 4, 7, 8, 9, and 10 (Karangsuraga, Pasauran, Pejamben, Tanjungjaya 1, and Tanjunglesung 1-3) have houses mixed with hotels, resorts, and villas. Sites 13, 15, 17, and 20 (Kertajaya Sumur, Bumi Waras, Wayurang 2, and Kunjir) have high-density housing. Sites 3, 6, 7, and 16 (Sukarame, Mekarsari, Tanjungjaya 1, and Wayurang 1) have agricultural land. Site 14 is a protected national park with limited access. Although this site has no residents, it is very important to review it because it includes the only Javan rhino (*Rhinoceros sondaicus*) habitat in the world. The Javan rhino is one of the most threatened mammals on earth, with a population of less than 100. The distribution of the rhino indicates that tsunamis are a significant risk to the species in the area (Setiawan et al., 2018).

Each site has a different beach profile. Most sites are natural beaches. Sites 2, 4, 8, 9, and 10 (Pasauran, Pejamben, and Tanjunglesung 1-3) have coastal structures (e.g., sea walls) and sites 5, 17, and 20 (Sukamaju, Wayurang 2, and Kunjir) have revetments.

5

Figure 1: Locations of field surveys. Sunda Strait lies between Java Island and Sumatra Island in Indonesia. Site numbers are followed by site names. Numbers in brackets indicate inundation distances and runup heights in meters, respectively

10 **Table 1**

Field survey sites and measurements

3 Method

15 Measurements of runup and inundation were conducted using conservative terrestrial surveying methods with optical and laser devices (e.g., total stations, handheld GPS devices, and laser distance meters). The maximum runup and inundation limits are based on remaining tsunami trail marks at measurement locations. The tracks were in the form of debris, fallen trees, plants that change color, and damage to buildings. The observed damage to buildings and structures was caused by the tsunami because there were no other causes, such as the earthquakes and liquefaction in the 2018 Sulawesi tsunami (Widiyanto et al., 2019). In addition, information regarding inundation limits and highest runup was also obtained from eyewitnesses. IOC 20 Manuals and Guides No. 37 (1998 and 2014) and field survey reports (Maramai and Tinti 1997; Farreras 2000; Matsutomi *et al.* 2001; Fritz and Okal 2008) were used as guidelines for the implementation of this field survey.

Sediment samples were collected from selected points at measurement locations that could be in the swash zone, nearshore, berm, or deposit areas (Table 2 and Fig. 2). The measurement of deposit thickness in sandy sheets was carried out by digging a number of shallow holes. The measured thickness was considered to be near the maximum thickness. This method was 25 qualitative and subjective because tsunami deposits are discontinuous, sporadic, and scattered over a flooded area. Sand sheets deposited on land vary greatly due to the influence of sedimentary sources and topography. A pit was made at each selected point to observe layers suspected to have been produced by the tsunami. We took only one sample at each pit for laboratory testing and did not take vertical samples at intervals of 1 cm, as done by some researchers (Gelfenbaum and Jaffe 2003; Hawkes *et al.* 2007; Srinivasalu *et al.* 2007; Srisutam and Wagner 2010), because a detailed analysis was not our focus, particularly 30 the number of tsunami waves and the vertical variation of sediment. The grain size of the samples obtained from the field was tested using ASTM standard sieve analysis. In addition, we investigated boulder movement at four sites.

Figure 2: Aerial photographs from Google Earth of transects including highest runup point and deposit pit.

35 **4 Runup**

The runup was measured by determining the height difference between the highest point of sea water rise onto land and the coastline. Runup is influenced by the characteristics of the ground surface and slope. The measurement results from our field surveys show that runup ranged from 1 to 8 m (Table 1 and Fig. 1). A runup height of about 1 m was found in many locations, at which no damage was found. The highest runup was found at the Cagar Alam, Kunjir, and Tanjung Jaya 2 sites, with heights 40 of 7.8, 7.7, and 7.0 m respectively. The Cagar Alam (sanctuary) site is part of the Ujung Kulon National Park. This site has a

flat topography and a dense forest. The guard post and water police office were completely destroyed by the tsunami. The Kunjir site, which is densely inhabited, had the second most victims after the Sumur site. This site is located on Sumatra Island about 38 km from the tsunami source. The Tanjung Jaya 2 site is a private resort with many tourists. The topography is relatively flat but suddenly rises at a distance of about 250 from the coastline due to a long hill. A large boulder moved by the tsunami was found at this site.

Figure 3: Positions of deposit pits and deposit limit compared to runup elevation.

5 Inundation

The distance from the runup point to the coastline is defined as the inundation distance (IOC Manuals and Guides No. 37, 2014). This distance can be easily obtained using a distance measurement instrument or GPS. We used total stations for this purpose. The results of our field measurements show that the inundation distance ranged from 10 to 290 m (Table 1 and Fig. 1). The wave with an inundation distance of 10 m and a runup of 1 m at site 15 (Bumi Waras) was not felt by the population. This site was chosen to represent the area of Bandarlampung City, which is the capital of Lampung Province. This city has a population of 1 million (2018) and must thus develop tsunami mitigation strategies. The longest inundation distance was found at site 14 (292.2 m), in the sanctuary, which also had the highest runup. At this site, measurements were made near the mouth of a small river. Long inundation distances may be caused by relatively flat topography with relatively few obstacles. Tsunami may also travel faster through a stream channel. A relatively long inundation (284.2 m) was also found at Tanjungjaya 2, a site with a relatively high runup. Fortunately, not many people live around this site other than at a resort complex, which suffered severe damage.

Figure 4: Positions of deposit pits and deposit limit compared to inundation distance.

6 Tsunami Wave Direction

The tsunami spread out from its source on the Anak Krakatau volcano to the beaches at the edge of Sunda Strait. To determine the direction of the tsunami that arrived at the beach, we obtained information from eyewitnesses. The tsunami hit at night and thus its arrival was difficult to see. Fortunately, it hit during a full moon period, so that there was some light. In addition to eyewitness accounts, we obtained evidence in the field related to the direction of the tsunami propagation. The evidence was in the form of fallen tree trunks, sloping vegetation and shrubs, damaged buildings, and building components carried away by the flow (Fig. 5).

Figure 5: Evidence of tsunami direction. Arrows show the direction of tsunami flow on the ground surfaces.

Our survey results show that the direction of the tsunami propagation was radial from the source (Fig. 6). The tsunami traveled east on the coast between Anyer and Labuhan (sites 1-6). In the vicinity of Tanjunglesung (sites 7-13), the tsunami was directed to the southeast, and in part of Ujung Kulon National Park (Site 14), the tsunami was directed southward. The tsunami was directed to the north and slightly to the northeast on Sumatra Island (sites 15-19). The westward tsunami toward the Tanggamus area was relatively small and insignificant. We did not include this area in the survey. The smaller magnitude of the tsunami to the west is likely due to obstruction by the island of Sertung and bathymetry factors. The Anak Krakatau mountain avalanche had a southwest direction, but the tsunami in this direction had no impact on human life because it leads to the open sea (the

Indian Ocean), with increasing depth from the tsunami source. Table 1 contains the quantity of tsunami wave direction arrived in coastal area. The direction ranges from 25° to 350° from north that it indicates radially propagation of the tsunami wave.

Figure 6: Direction of tsunami propagation, the tsunami spread radially from its source.

5

7 Sediment Characteristics

7.1 Tsunami Deposits

Prehistoric (paleo-) tsunamis have been identified from sediment deposits (Atwater 1992; Dawson and Shi 2000; Peters, Jaffe and Gelfenbaum 2007). Sediment deposits can be used to explain and reconstruct significant tsunami events (Dawson *et al.* 1995; Van Den Bergh *et al.* 2003). The present study attempts to describe the impact of a recent tsunami on sediment movement around the coastal area. The tsunami carried sediment from the coast inland. However, not all sites that we measured had significant sediment deposits. Only places with a sufficient source of material had clearly observable sediment deposits (Fig. 7). The survey sites used for sediment samples are shown in Fig. 2. Sediment deposits generally do not spread evenly and continuously but are separated at certain locations, which allow it to settle. Topography controls sediment deposits; for instance, there are more sediment deposits at ground surface depressions.

Figure 7: Tsunami sediment deposit, test pits were made to measure the deposit thickness.

The best location for the observation of tsunami sediment is about 50-200 m inland from the coastline (Srisutam and Wagner, 2010) or about 50-400 m inland (Moore et al., 2006), as used for the 2004 Sumatra-Andaman tsunami. In this study, the 12 deposit pits were 15-200 m (average: 93 m) from the shoreline. Four deposit pits were less than 50 m from the shoreline (11). Three of them were at sites 1, 2, and 7, respectively, due to the short inundation and beach scarp. Another was at site 13 (Kertajaya Sumur), where high-density housing blocked the sediment transport and created a deposit a short distance from the shoreline.

The interpretation of tsunami magnitude, especially runup and inundation based on tsunami deposits, is challenging (Dawson and Shi 2000). However, the relationship between deposits and runup or inundation is still not convincing because of the high variability of tsunami deposits in terms of thickness and location. Soulsby et al. (2007) proposed a mathematical model for reconstructing tsunamis runup from sedimentary characteristics. The runup distance for sediment is related to the runup distance for water as:

$$R_s = \frac{R_w}{1+\alpha\gamma} \quad (1)$$

where R_s is the maximum distance inland for sediment deposition, R_w is the runup limit for water, α is as shown in Eq. 2, and γ is a comparison factor between uprush time and total uprush plus backwash time.

$$\alpha = \frac{w_s T}{H} \quad (2)$$

where w_s is the settling velocity, T is a period from the time of first wetting to final drying of inundated ground, and H is the tsunami height. 11 shows the measured sediment runup and water runup compared to the theoretical sediment runup; the results are in good agreement.

The sediment samples were tested for gradations in the laboratory. The results for each site are shown in Fig. 9. The sediment in the deposit areas on land is generally finer than at the sources at the beach (nearshore or swash zone). The characteristics of the sediment are discussed in Section 7.3. The sediment deposition thickness varied greatly from one point to another at the

survey sites. We chose a test pit with significant thickness for sampling. The thickness was likely near the maximum sediment thickness in the area.

5

7.2 Boulder Movement

Coastal boulder accumulation is usually associated with high-energy events (tsunamis, hurricanes, or powerful storms). A characteristic of many tsunamis is their ability to deposit boulders across the coastal zone (Dawson and Shi, 2000). Extreme storms also have the ability to deposit boulders (Morton, Gelfenbaum and Jaffe 2007; Richmond *et al.* 2010). The interpretation of boulders is difficult along coasts where both storms and tsunamis have occurred. We identified boulders moved by a tsunami wave and runup at three survey sites based on information from eyewitnesses and their physical state. Eyewitnesses said that these boulders were in new positions after the tsunami. In addition, from the physical criteria given by Morton *et al.* (2007) and Paris *et al.* (2010), it was most likely that the boulders were moved by the tsunami. At about the time of the tsunami event, a tropical cyclone called Kenanga formed in the Indian Ocean about 1400 km from Sunda Strait. Kenanga had a speed of 75 km/h and was active from December 15 to 18, 2018 (Prabowo, 2018). The influence of this cyclone was weak in the coastal zone, and thus it was unlikely to have moved the boulders.

The largest boulder, measuring 2.7 m in diameter (10.4 tons), was found at site 11 (Tanjungjaya 2), as shown in Fig. 8a. This boulder moved from its original point in the swash zone to 81 m inland. Other smaller stones were scattered around it. In Tanjunglesung (sites 8, 9, and 10), pebbles, cobbles, and small boulders (25-50 cm) were scattered up to 40 m from the coastline. At site 4, the seawall built to protect a hotel and villas was partly destroyed and moved ashore. A seawall chunk, measuring 1 m × 1 m × 4.2 m (9.5 tons), made from rubble mound and mortar moved as far as 30 m from its place of origin (Fig. 8b). Other smaller chunks also moved.

Figure 8: (a) Boulder that moved around 82 m inland and (b) an element of seawall that moved around 30 m inland.

25

The characteristics of the boulders moved by a tsunami can be used to estimate the associated flow velocities. For instance, the 2004 tsunami had flow velocities of 3-13 m/s. This tsunami drove a 7.7-ton calcareous boulder 200 m and an 11-ton coral boulder as far as 900 m (Paris *et al.*, 2010). The velocity was calculated as:

$$u = \sqrt{\left(\frac{2\mu mg}{C_d A_n \rho_w}\right)} \quad (3)$$

where μ is the friction coefficient, m is the boulder mass (kg), g is the gravitational acceleration, C_d is the drag coefficient, A_n is the area of the boulder projected normal to the flow (m^2), and ρ_w is the density of sea water. The velocities were calculated to be $u \geq 4.5$ m/s and $u \geq 4.0$ m/s for the 10.4-ton (Fig. 8a) and 9.4-ton (Fig. 8b) boulders, respectively.

7.3 Sand Size Statistics

The results of sieve analysis, namely sand grain size distributions, are shown as a cumulative distribution curve of sand grain size. Fig. 9 shows the cumulative distribution curve for 12 sites. From the curve, various diameter values were determined, including d_{95} , d_{84} , d_{50} , d_{16} , and d_5 . From these diameters, other statistics can be determined, namely the mean, standard deviation, skewness, and kurtosis (Table 2). The mean can be used for grain size classification. The standard deviation is a measure of range that shows the uniformity of a sand sample. A perfectly sorted sample will have sand of the same diameter, whereas poorly sorted sand will have a wide size range. Beach sand size distributions with a standard deviation of ≤ 0.5 are considered well sorted, and those with a standard deviation of ≥ 1 are assumed to be poorly sorted. Skewness occurs when the sand size distribution is not symmetrical. A negative skewness value indicates that the distribution is tending to the value of

small phi (large grain size). Kurtosis determines the peakedness of the size distribution. The normal distribution has a kurtosis value of 0.65. If the distribution is more diffuse and wider than the normal distribution, the kurtosis value will be less than 0.65 (Dean and Dalrymple 2004).

5 **Figure 9: Sediment grain size results from sieve analysis for various sites.**

From our results, the mean values show that medium and coarse were the dominant types of sand in the sample. Very coarse sand, granular sand, and pebbles were found at the Tanjungjaya 2 and Sukarame sites. Fine and very fine sand was also identified at several sites. The range of grain sizes found in the study area depended on the available source material.

10 Wentworth classification was used to assess the grain size. All samples had negative standard deviations, indicating that they had well sorted distributions.

Table 2 Sediment statistics and characteristics

15 7 of the 10 samples taken from the swash zone had negative skewness, which indicated a large phi value and an erosive tendency in the zone. The numbers of samples with positive and negative skewness were similar (7 and 6, respectively). Some deposit samples were taken at a distance of less than 50 m from the coastline, which may still be an erosive environment.

The kurtosis of the tsunami sediment indicates that grain size distributions were flat to peaked distribution. Generally, the major sources of tsunami sediment are swash zones and berm/dune zone sands, where coarse to medium sands are dominant.

20 A minor source of tsunami sediment is the shoreface, where fine to very fine sands are dominant. However, for a coastal area where the shoreface slope is mild, the major source of tsunami sediment is the shoreface. Table 2 provides kurtosis values from which distribution of sediment range from very platykurtic to very leptokurtic.

8 Conclusion

We selected 20 sites on Java Island and Sumatra Island to observe the impact of the December 2018 tsunami, which was
25 caused by a mass movement of an Anak Krakatau volcano flank. The survey results revealed that the runup height ranged from 1 to 8 m, the inundation distance was 10 to 300 m, and the direction of the tsunami was between 25° and 350°. The highest runup (7.8 m) and the longest inundation distance (292 m) were found at site 14 (Cagar Alam), which contains a forest area, part of a national park, and a UNESCO heritage site. Sediment samples were taken from 27 points in tsunami deposits with a sediment thickness of 1.5-12 cm. The distance of area with significant sediment deposits caused by the tsunami from the coast
30 varied in the range of 15-200 m (average: 93 m) from the shoreline or 40%-90% (average: 67%) of the inundation distance. The elevations of the significant sediment deposits reached 60%-90% (average: 81%) of the runup elevation. Sediment material larger than coarse sand (granular sand, pebbles, cobbles, and boulders) was found at several locations. The largest boulder had a diameter of 2.7 m and a weight of 10.4 tons. From the boulder movement, the tsunami velocity at the ground surface was estimated to be more than 4.5 m/s. Sand size statistics were also given in this report. The sediment grain size ranged from very
35 fine sand to boulders, with medium sand (diameter: 0.25-0.5 mm) and coarse sand (diameter: 0.5 -1.0 mm) being dominant. All sediment samples tested in the laboratory had a well sorted distribution, indicating that the grain sizes were relatively uniform.

Acknowledgment

This study was funded by the Ministry of Science and Technology, Taiwan, under grant MOST 107-2221-E-006-080 and the
40 Water Resources Agency, MOEA, under grant MOEAWRA 1080412. The authors would like to thank the Geomatics

Laboratory and the Soil Mechanics Laboratory at the Civil Engineering Department, Universitas Jenderal Soedirman, Purwokerto, Indonesia. We would also like to thank Ujung Kulon National Park and Tanjung Lesung Special Economic Zone for conducting surveys in their areas. We are grateful to Mr. Sumantri from Tanjunglesung Special Economic Zone and Mr. Budi from Carita Resort for accompanying the tsunami impact review and providing detailed chronological information on the tsunami, especially in Tanjunglesung and Carita Beach, respectively. We appreciate Mrs. Sanidhya Nika Purnomo for discussion on geographical information.

References

- Atwater, B. F.: Geologic evidence for earthquakes during the past 2000 years along the Copalis River, southern coastal Washington, *J. Geophys. Res. Solid Earth*, 97(B2), 1901–1919, doi:10.1029/91jb02346, 1992.
- 10 Van DenBergh, G. D., Boer, W., DeHaas, H., VanWeering, T. C. E. andVanWijhe, R.: Shallow marine tsunami deposits in Teluk Banten (NW Java, Indonesia), generated by the 1883 Krakatau eruption, *Mar. Geol.*, 197(1–4), 13–34, doi:10.1016/S0025-3227(03)00088-4, 2003.
- Camus, G., Diament, M., Gloaguen, M., Provost, A. andVincent, P.: Emplacement of a Debris Avalanche during the 1883 eruption of Krakatau (Sunda Straits, Indonesia), *GeoJournal*, 28(2), 123–128, doi:10.1007/BF00177224, 1992.
- 15 Dawson, A. G. andShi, S.: Tsunami Deposits, *Pure appl. Geophys*, 157, 875–897, 2000.
- Dawson, A. G., Hindson, R., Andrade, C., Freitas, C. andParish, R.: Tsunami sedimentation associated with the Lisbon earthquake of 1 November AD 1755 Boca do Rio, Algarve, Portugal, *The Holocene*, 5(2), 209–215, 1995.
- Dean, R. G. andDalrymple, R. A.: *Coastal Processes with Engineering Application*, 1st ed., Cambridge University Press, Cambridge., 2004.
- 20 Farreras, S. F.: Post-tsunami field survey procedures: An outline, *Nat. Hazards*, 21(2–3), 207–214, doi:10.1023/A:1008049228148, 2000.
- Fritz, H. M. andOkal, E. A.: Socotra Island, Yemen: Field survey of the 2004 Indian Ocean tsunami, *Nat. Hazards*, 46(1), 107–117, doi:10.1007/s11069-007-9185-3, 2008.
- Gelfenbaum, G. andJaffe, B.: Erosion and sedimentation from the 17 July, 1998 Papua New Guinea tsunami, *Pure Appl. Geophys.*, doi:10.1007/s00024-003-2416-y, 2003.
- 25 Giachetti, T., Paris, R., Kelfoun, K. andOntowirjo, B.: Tsunami hazard related to a flank collapse of Anak Krakatau Volcano, Sunda Strait, Indonesia, *Geol. Soc. London, Spec. Publ.*, 361(1), 79–90, doi:10.1144/sp361.7, 2012.
- Hawkes, A. D., Bird, M., Cowie, S., Grundy-Warr, C., Horton, B. P., Shau Hwai, A. T., Law, L., Macgregor, C., Nott, J., Ong, J. E., Rigg, J., Robinson, R., Tan-Mullins, M., Sa, T. T., Yasin, Z. andAik, L. W.: Sediments deposited by the 2004 Indian Ocean Tsunami along the Malaysia–Thailand Peninsula, *Mar. Geol.*, doi:10.1016/j.margeo.2007.02.017, 2007.
- 30 IOC Manuals and Guides No. 37: *International Tsunami Survey Team (ITST) Post-Tsunami Survey Field Guide*, 2nd ed., edited by D.Dominey-Howes, L.Dengler, J.Cunnen, andT.Aarup, the United Nations Educational, Scientific and Cultural Organization, Paris., 2014.
- Kasbani: *Pers Rilis Aktivitas Gunung Anak Krakatau*, 28 Desember 2018, 2018.
- 35 Maeno, F. andImamura, F.: Tsunami generation by a rapid entrance of pyroclastic flow into the sea during the 1883 Krakatau eruption, Indonesia, *J. Geophys. Res. Solid Earth*, 116(9), 1–24, doi:10.1029/2011JB008253, 2011.
- Maramai, A. andTinti, S.: The 3 June 1994 Java Tsunami: A post-event survey of the coastal effects, *Nat. Hazards*, doi:10.1023/A:1007957224367, 1997.
- Matsutomi, H., Shuto, N., Imamura, F. andTakahashi, T.: Field survey of the 1996 Irian Jaya earthquake Tsunami in Biak Island, *Nat. Hazards*, 24(3), 199–212, doi:10.1023/A:1012042222880, 2001.
- 40 Moore, A., Nishimura, Y., Gelfenbaum, G., Kamataki, T. andTriyono, R.: Sedimentary deposits of the 26 December 2004

- tsunami on the northwest coast of Aceh, Indonesia, *Earth Planets Sp.*, 58, 253–258, 2006.
- Morton, R. A., Gelfenbaum, G. and Jaffe, B. E.: Physical criteria for distinguishing sandy tsunami and storm deposits using modern examples, *Sediment. Geol.*, doi:10.1016/j.sedgeo.2007.01.003, 2007.
- Paris, R., Fournier, J., Poizot, E., Etienne, S., Morin, J., Lavigne, F. and Wassmer, P.: Boulder and fine sediment transport and deposition by the 2004 tsunami in Lhok Nga (western Banda Aceh, Sumatra, Indonesia): A coupled offshore-onshore model, *Mar. Geol.*, doi:10.1016/j.margeo.2009.10.011, 2010.
- Paris, R., Wassmer, P., Lavigne, F., Belousov, A., Belousova, M., Iskandarsyah, Y., Benbakkar, M., Ontowirjo, B. and Mazzoni, N.: Coupling eruption and tsunami records: The Krakatau 1883 case study, Indonesia, *Bull. Volcanol.*, 76(4), 1–23, doi:10.1007/s00445-014-0814-x, 2014.
- Peters, R., Jaffe, B. and Gelfenbaum, G.: Distribution and sedimentary characteristics of tsunami deposits along the Cascadia margin of western North America, *Sediment. Geol.*, doi:10.1016/j.sedgeo.2007.01.015, 2007.
- Prabowo, M. R.: Siklon Tropis “Kenanga” Tumbuh di Samudra Hindia Selatan Sumatera, *bmkg.go.id*, 2018.
- Richmond, B. M., Buckley, M., Gelfenbaum, G., Morton, R. A., Watt, S. and Jaffe, B. E.: Recent storm and tsunami coarse-clast deposit characteristics, southeast Hawai‘i, *Mar. Geol.*, doi:10.1016/j.margeo.2010.08.001, 2010.
- Setiawan, R., Gerber, B. D., Rahmat, U. M., Daryan, D., Firdaus, A. Y., Haryono, M., Khairani, K. O., Kurniawan, Y., Long, B., Lyet, A., Muhiban, M., Mahmud, R., Muhtarom, A., Purastuti, E., Ramono, W. S., Subrata, D. and Sunarto, S.: Preventing Global Extinction of the Javan Rhino: Tsunami Risk and Future Conservation Direction, *Conserv. Lett.*, 11(1), doi:10.1111/conl.12366, 2018.
- Srinivasalu, S., Thangadurai, N., Switzer, A. D., Ram Mohan, V. and Ayyamperumal, T.: Erosion and sedimentation in Kalpakkam (N Tamil Nadu, India) from the 26th December 2004 tsunami, *Mar. Geol.*, doi:10.1016/j.margeo.2007.02.003, 2007.
- Srisutam, C. and Wagner, J. F.: Tsunami sediment characteristics at the Thai Andaman Coast, *Pure Appl. Geophys.*, doi:10.1007/s00024-009-0015-2, 2010.
- Verbeek, R. D. M.: The Krakatoa Eruption, *Nature*, 10–15, 1884.
- Widiyanto, W., Santoso, P. B., Hsiao, S.-C. and Imananta, R. T.: Post-event Field Survey of 28 September 2018 Sulawesi Earthquake and Tsunami, *Nat. Hazards Earth Syst. Sci. Discuss.*, (September 2018), 1–23, doi:10.5194/nhess-2019-91, 2019.
- Yokoyama, I.: A scenario of the 1883 Krakatau tsunami, *J. Volcanol. Geotherm. Res.*, 34(1–2), 123–132, doi:10.1016/0377-0273(87)90097-7, 1987.

30

35

40

Table 1 Field survey sites and measurements

Site	Site name	Measurement time	Coordinates		Inundation distance (m)	Runup height (m)	Tsunami direction from North (°)	Sediment sample numbers
			Long. (°)	Lat. (°)				
1	Karangsuraga	25 Jan 2019	-6.148434	105.854718	84.00	4.7	82	S-01, S-02
2	Pasauran	25 Jan 2019	-6.202289	105.836179	111.00	5.8	84	S-03, S-04
3	Sukarame	24 Jan 2019	-6.261508	105.830448	204.66	4.1	93	S-05, S-06, S-07
4	Pejamben	24 Jan 2019	-6.316783	105.831298	200.80	5.0	105	-
5	Sukamaju	24 Jan 2019	-6.390917	105.825965	125.85	2.2	110	-
6	Mekarsari	25 Jan 2019	-6.520795	105.758381	123.80	2.3	115	S-08
7	Tanjungjaya 1	27 Jan 2019	-6.509201	105.673902	60.57	1.1	210	S-09, S-10
8	Tanjunglesung 1	23 Jan 2019	-6.480980	105.659513	149.54	3.4	135	S-11, S-12, S-13
9	Tanjunglesung 2	23 Jan 2019	-6.480914	105.654575	202.17	3.6	128	-
10	Tanjunglesung 3	23 Jan 2019	-6.481270	105.652097	177.06	2.4	133	S-14, S-15, S-16
11	Tanjungjaya 2	23 Jan 2019	-6.504584	105.642052	284.17	7.0	120	S-17, S-18, S-19
12	Banyuasih	23 Jan 2019	-6.600539	105.621017	170.30	2.1	142	-
13	Kertajaya Sumur	26 Jan 2019	-6.656894	105.583253	134.68	5.0	150	S-20, S-21
14	Cagar Alam	26 Jan 2019	-6.676569	105.378788	292.19	7.8	180	S-22, S-23, S-24
15	Bumi Waras	28 Jan 2019	-5.459514	105.262263	10.00	1.1	350	-
16	Wayurang 1	28 Jan 2019	-5.72307	105.582329	181.58	4.2	30	S-25, S-26, S-27
17	Wayurang 2	28 Jan 2019	-5.745806	105.587961	81.34	4.2	34	-
18	Kotaguring	28 Jan 2019	-5.800583	105.584414	29.07	2.6	25	-
19	Sukaraja	28 Jan 2019	-5.833699	105.626956	64.44	2.4	40	-
20	Kunjir	28 Jan 2019	-5.834768	105.642150	207.13	7.7	47	-

5

10

15

Table 2 Sediment statistics and characteristics

Sample	Date (dd/mm/yy)	Time (+8 UTC	Lat. (°S)	Long. (°E)	Village	Subdistrict	Regency	Zone	Deposit thickness (cm)	Median D ₅₀ (mm)	Φ ₅₀	Mean	Std. Dev.	Skew- ness	Kurto- sis	Remarks
S-01	25/01/19	16:30:38	-6.148187	105.854549	Karangsuraga	Cinangka	Serang	swash zone	-	0.650	0.621	0.883	-1.368	-0.191	-0.864	coarse sand, well sorted, very platykurtic
S-02	25/01/19	16:45:44	-6.148195	105.854774	Karangsuraga	Cinangka	Serang	deposit	12	0.330	1.599	1.698	-0.698	-0.141	0.504	medium sand, well sorted, very platykurtic
S-03	25/01/19	15:02:22	-6.202145	105.835194	Pasauran	Cinangka	Serang	swash zone	-	0.200	2.322	0.007	-2.177	1.063	0.536	coarse sand, well sorted, very platykurtic
S-04	25/01/19	15:19:01	-6.201856	105.835437	Pasauran	Cinangka	Serang	deposit	3	0.500	1.000	0.652	-1.237	0.281	0.603	coarse sand, well sorted, very platykurtic
S-05	24/01/19	16:44:32	-6.260923	105.828634	Sukarame	Labuhan	Pandeglang	nearshore	-	3.000	-1.585	-1.243	-1.757	-0.195	0.463	granular, well sorted, very platykurtic
S-06	24/01/19	16:49:13	-6.261013	105.828977	Sukarame	Labuhan	Pandeglang	swash zone	-	0.500	1.000	0.921	-0.769	0.103	0.599	coarse sand, well sorted, very platykurtic
S-07	24/01/19	16:54:01	-6.261021	105.829628	Sukarame	Labuhan	Pandeglang	deposit	6.3	0.500	1.000	0.268	-1.368	0.461	0.579	coarse sand, well sorted, very platykurtic
S-08	25/01/19	18:54:59	-6.520795	105.758381	Mekarsari	Panimbang	Pandeglang	deposit	12.7	0.330	1.599	1.656	-0.740	-0.076	0.497	medium sand, well sorted, very platykurtic
S-09	27/01/19	08:34:50	-6.509219	105.674029	Tanjungjaya 1	Panimbang	Pandeglang	swash zone	-	0.240	2.059	1.994	-0.743	0.087	1.516	medium sand, well sorted, very leptokurtic
S-10	27/01/19	08:35:35	-6.509201	105.672903	Tanjungjaya 1	Panimbang	Pandeglang	deposit	2	0.650	0.621	0.128	-1.561	0.316	0.550	coarse sand, well sorted, very platykurtic
S-11	23/01/19	12:22:32	-6.479796	105.658553	Tanjunglesung 1	Panimbang	Pandeglang	swash zone	-	0.220	2.184	2.266	-0.792	-0.103	0.790	fine sand, well sorted, platykurtic
S-12	23/01/19	12:15:53	-6.480013	105.658580	Tanjunglesung 1	Panimbang	Pandeglang	deposit	3	0.170	2.556	2.791	-1.005	-0.233	0.715	fine sand, well sorted, platykurtic
S-13	23/01/19	12:32:23	-6.480799	105.659432	Tanjunglesung 1	Panimbang	Pandeglang	deposit	1.5	0.260	1.943	1.808	-0.749	0.181	1.730	medium sand, well sorted, very leptokurtic
S-14	23/01/19	10:52:19	-6.480284	105.652178	Tanjunglesung 3	Panimbang	Pandeglang	swash zone	-	0.400	1.322	1.630	-0.844	-0.365	0.722	medium sand, well sorted, very leptokurtic
S-15	23/01/19	11:04:00	-6.480438	105.652278	Tanjunglesung 3	Panimbang	Pandeglang	deposit	6.8	0.410	1.286	1.117	-0.883	0.192	1.936	medium sand, well sorted, very leptokurtic
S-16	23/01/19	11:53:24	-6.481134	105.652333	Tanjunglesung	Panimbang	Pandeglang	deposit	3.2	0.380	1.396	1.619	-0.703	-0.317	2.008	medium sand, well sorted, very leptokurtic
S-17	23/01/19	14:28:44	-6.503221	105.639871	Tanjungjaya 2	Panimbang	Pandeglang	nearshore	-	4.200	-2.070	-2.276	-1.074	0.191	0.365	pebble, well sorted, very platykurtic
S-18	23/01/19	14:38:08	-6.502949	105.640477	Tanjungjaya 2	Panimbang	Pandeglang	swash zone	-	1.200	-0.263	-0.026	-1.460	-0.163	0.332	very coarse sand, well sorted, very platykurtic
S-19	23/01/19	14:51:05	-6.504377	105.641338	Tanjungjaya 2	Panimbang	Pandeglang	deposit	-	0.380	1.396	1.429	-0.893	-0.037	0.588	medium sand, well sorted, very platykurtic
S-20	26/01/19	18:40:59	-6.655898	105.583705	Kertajaya	Sumur	Pandeglang	swash zone	-	0.950	0.074	0.465	-1.272	-0.037	0.778	coarse sand, well sorted, platykurtic
S-21	26/01/19	14:42:08	-6.656034	105.583687	Kertajaya	Sumur	Pandeglang	deposit	2	0.220	2.184	1.826	-0.911	0.393	1.131	medium sand, well sorted, leptokurtic
S-22	26/01/19	12:27:00	-6.673185	105.379727	Cagar Alam	Sumur	Pandeglang	nearshore	-	0.220	2.184	1.800	-0.937	0.410	1.654	medium sand, well sorted, very leptokurtic
S-23	26/01/19	13:14:17	-6.674877	105.379122	Cagar Alam	Sumur	Pandeglang	swash zone	-	0.380	1.396	1.494	-0.828	-0.119	1.071	medium sand, well sorted, mesokurtic
S-24	26/01/19	14:03:24	-6.675483	105.378968	Cagar alam	Sumur	Pandeglang	deposit	7.5	0.120	3.059	3.020	-0.624	0.063	0.861	very fine sand, well sorted, platykurtic
S-25	28/01/19	14:04:46	-5.724157	105.581636	Wayurang	Kalianda	S. Lampung	nearshore	-	0.190	2.396	2.370	-0.814	0.031	0.697	fine sand, well sorted, platykurtic
S-26	28/01/19	13:48:51	-5.723089	105.581996	Wayurang	Kalianda	S. Lampung	swash zone	-	0.190	2.396	2.398	-0.660	-0.003	0.995	fine sand, well sorted, mesokurtic
S-27	28/01/19	14:04:46	-5.724157	105.581636	Wayurang	Kalianda	S. Lampung	deposit	12.3	0.170	2.556	2.959	-0.930	-1.718	-2.248	coarse sand, well sorted, very platykurtic

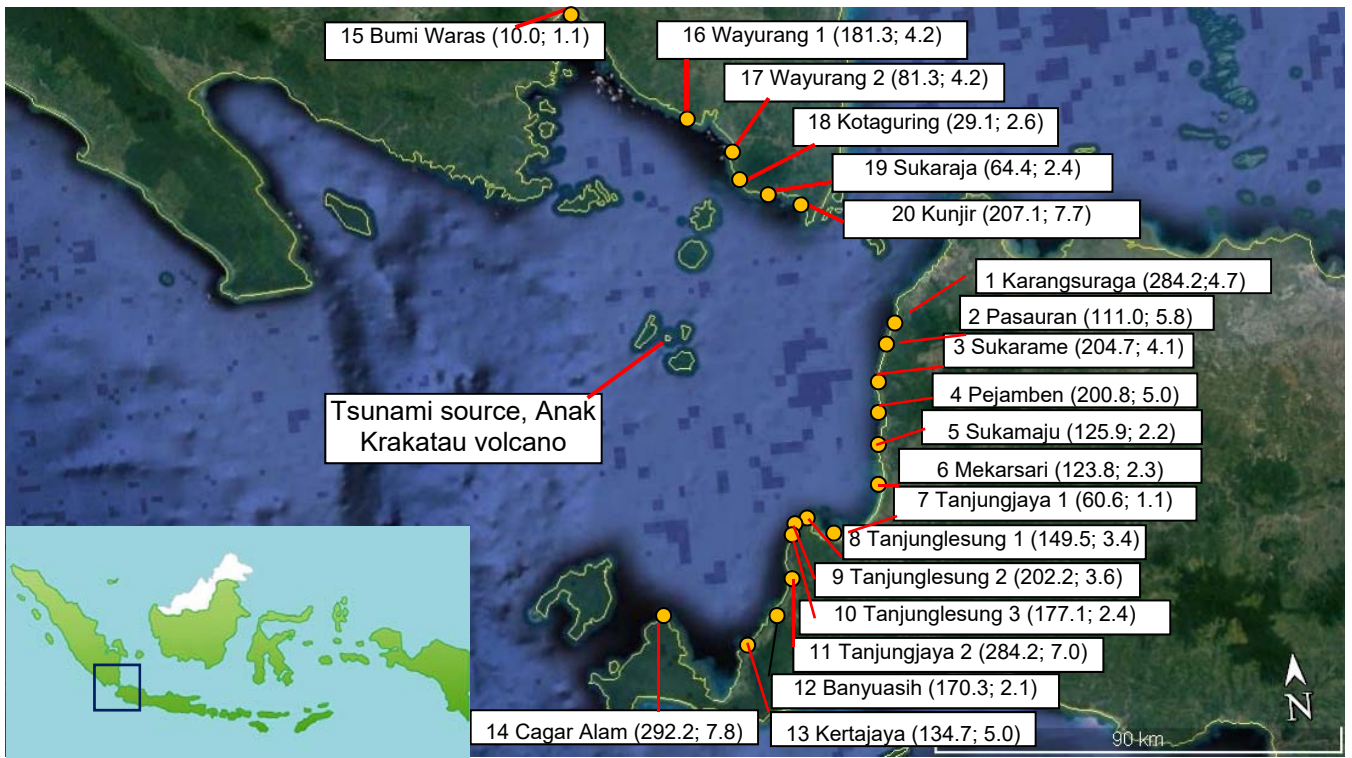


Figure 1: Locations of field surveys. Sunda Strait lies between Java Island and Sumatra Island in Indonesia. Site numbers are followed by site names. Numbers in brackets indicate inundation distances and runup heights in meters, respectively.

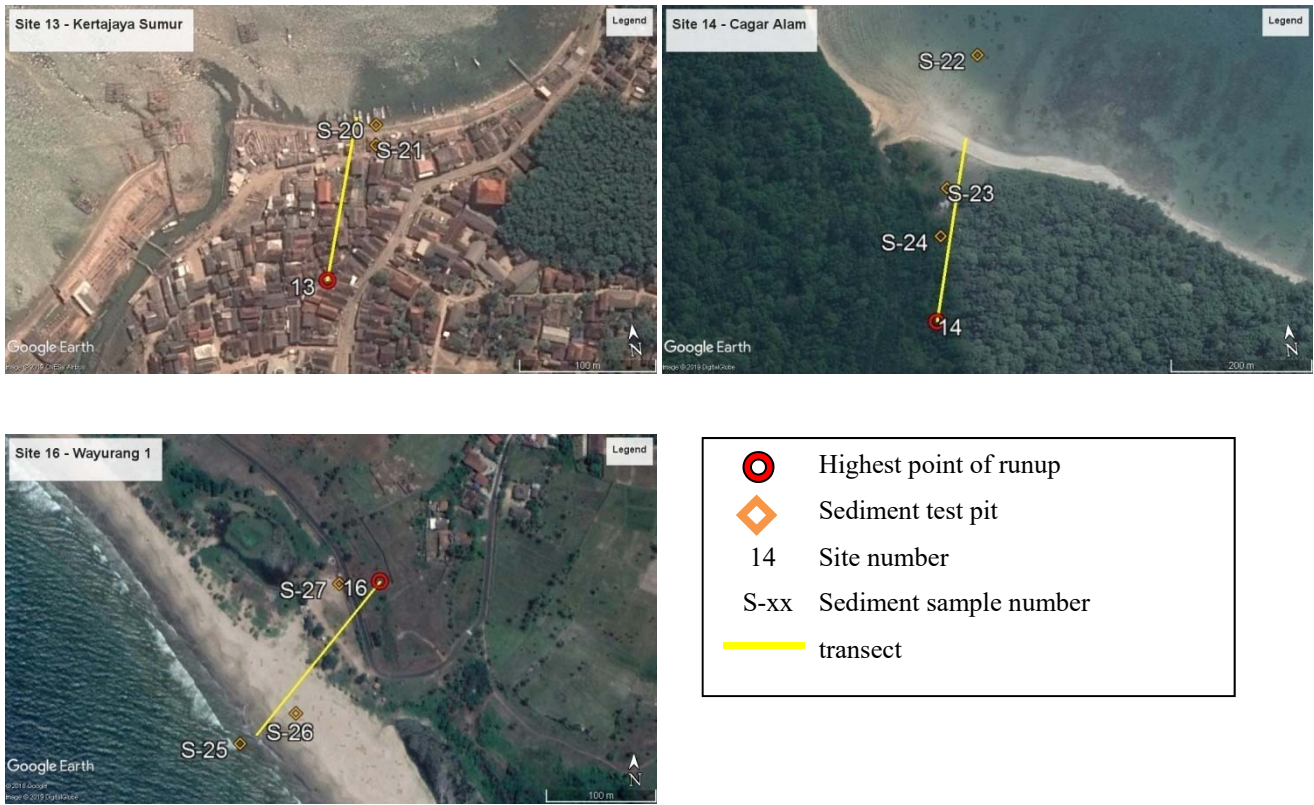
5

10

15



5



5 Figure 2: Aerial photographs from Google Earth of transects including highest runup point and deposit pit.

10

15

20

25

5



Figure 3: Evidence of tsunami direction. Arrows show the direction of tsunami flow on the ground surfaces.

10

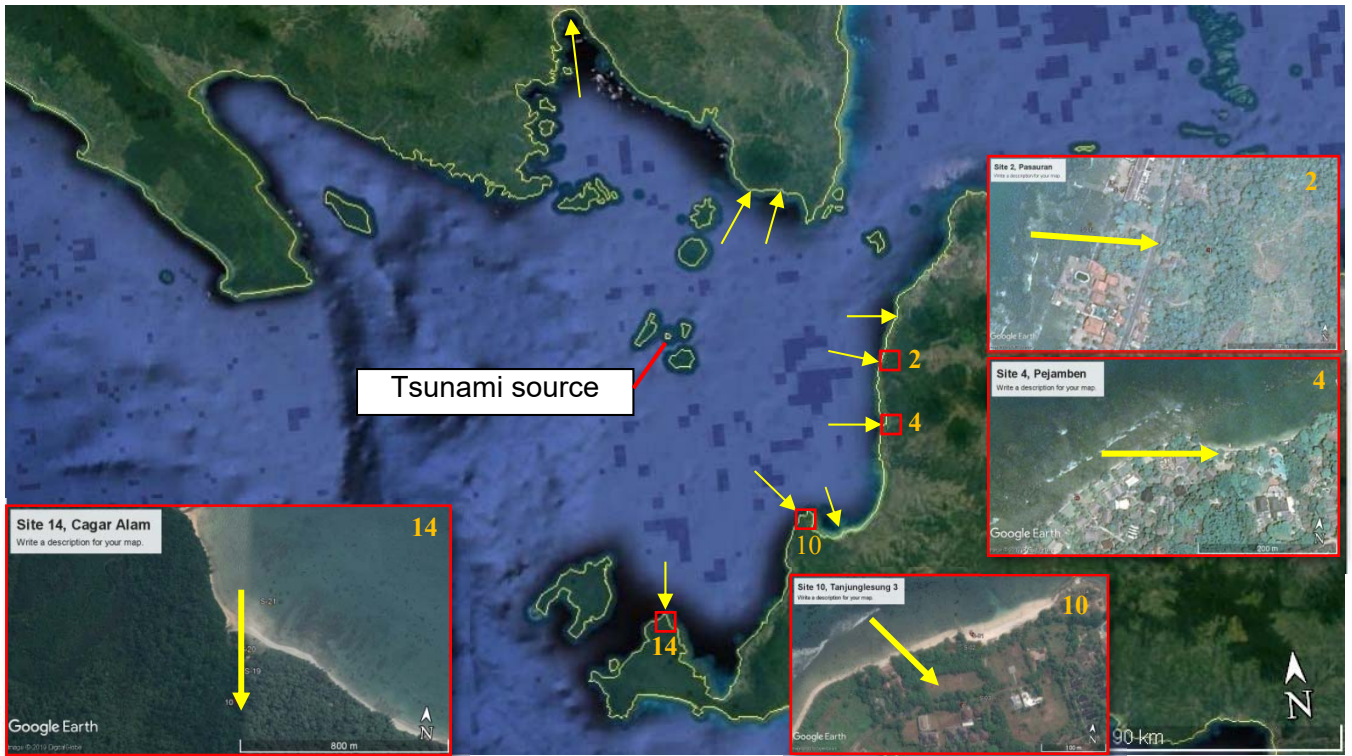


Figure 4: Direction of tsunami propagation, the tsunami spread radially from its source.

5



Figure 5: Tsunami sediment deposit, test pits were made to measure the deposit thickness.

10

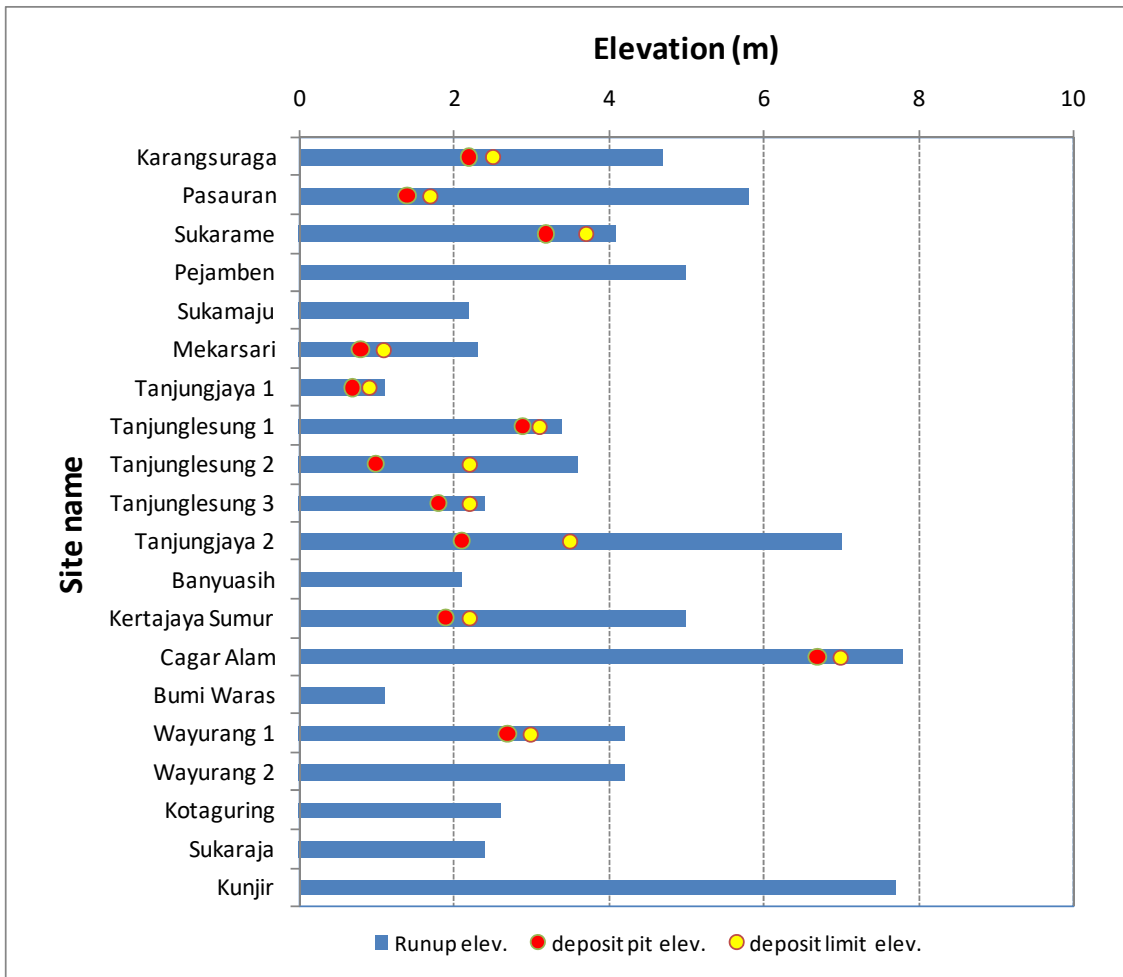


Figure 6: Positions of deposit pits and deposit limit compared to runup elevation

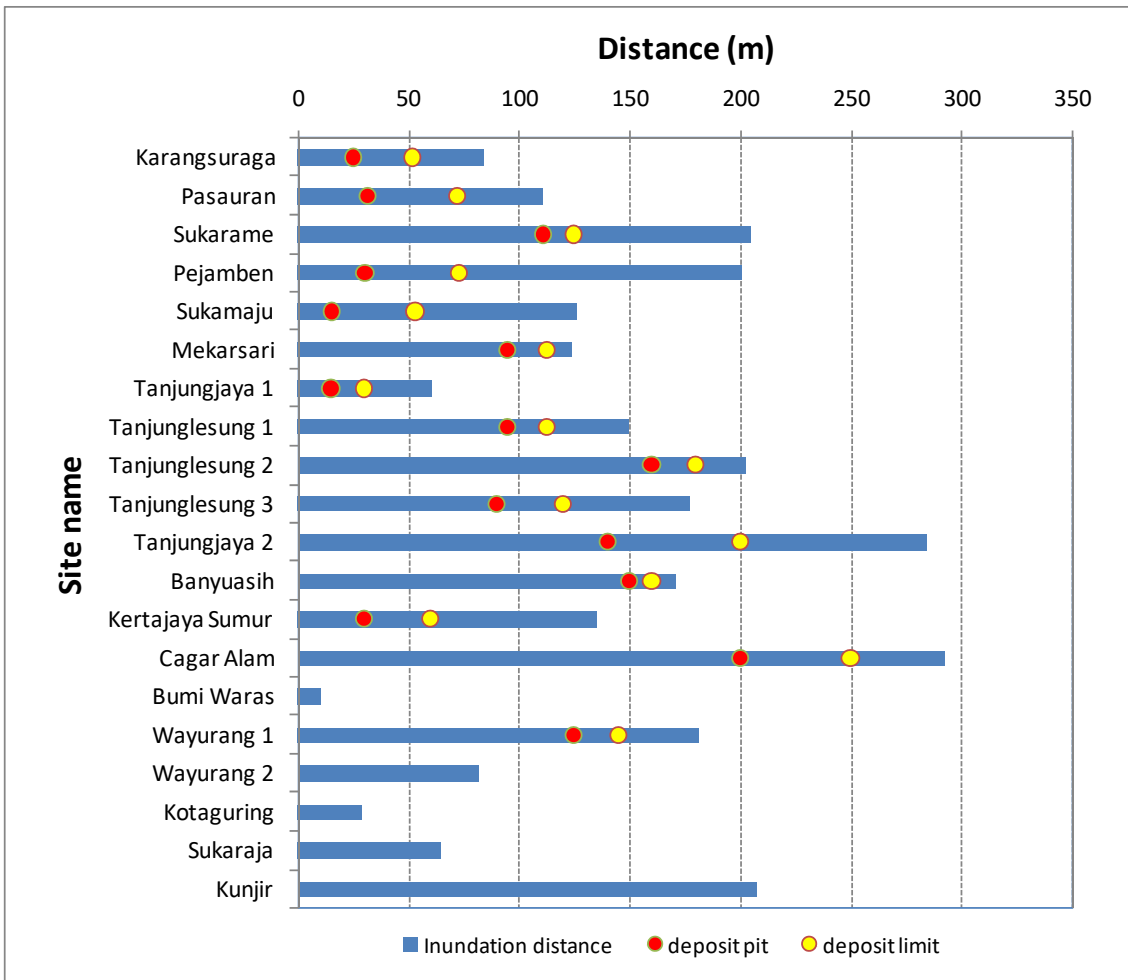
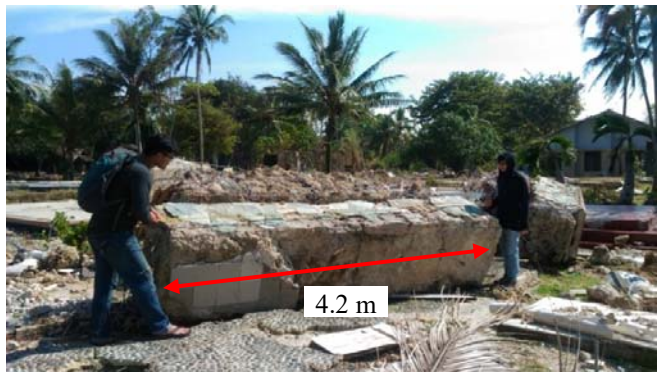


Figure 7: Positions of deposit pits and deposit limit compared to inundation distance.

5



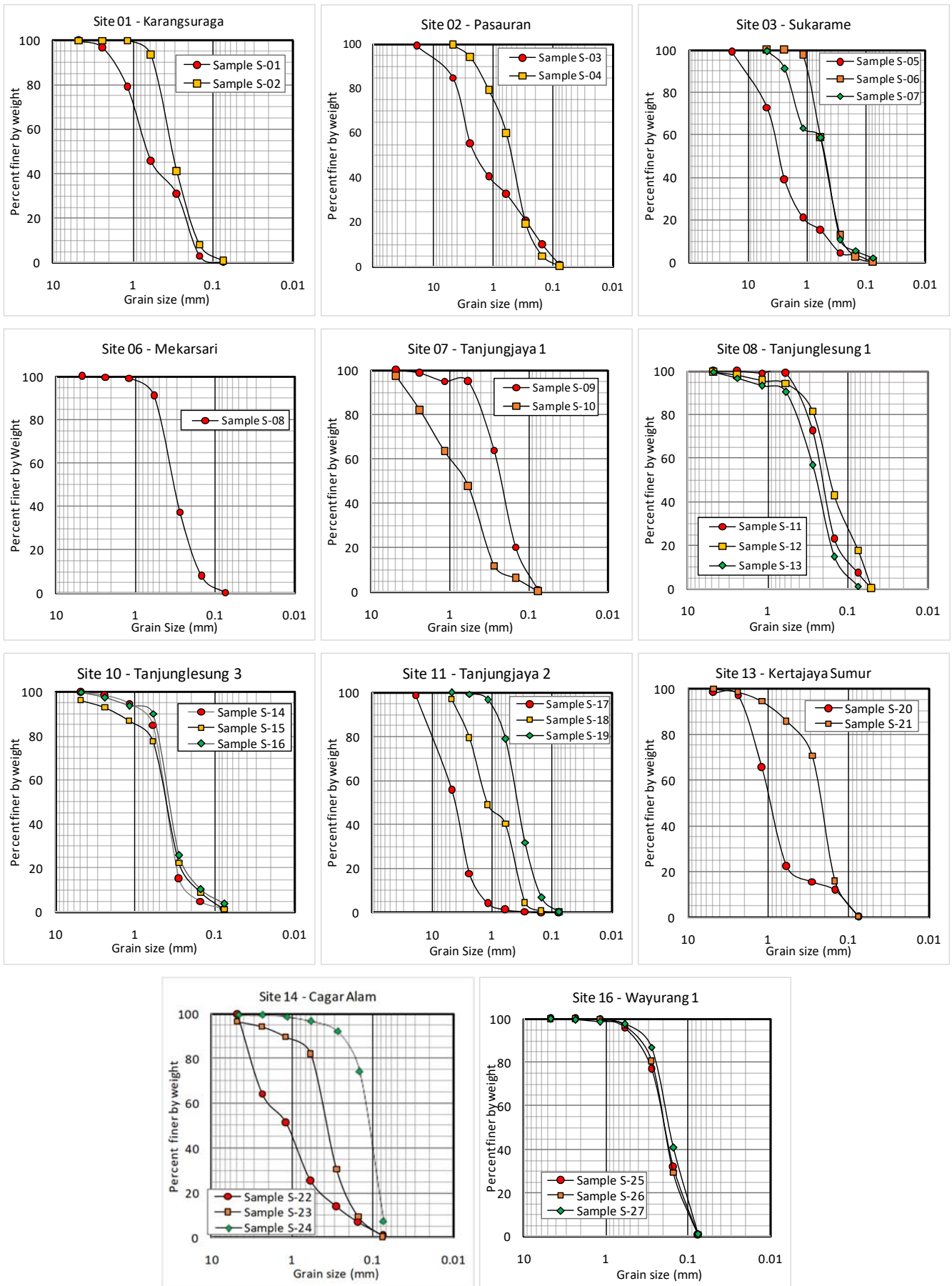
(a)



(b)

Figure 8: (a) Boulder that moved around 82 m inland and (b) an element of seawall that moved around 30 m inland.

10



5 Figure 9: Sediment grain size results from sieve analysis for various sites.